Applied Mathematics and Computation 530 (2026) 130156

Contents lists available at ScienceDirect

Applied Mathematics and Computation

journal homepage: www.elsevier.com/locate/amc

Full Length Article

A stochastic dengue transmission model: Noise-induced extinction and optimal control

Anita Mandal [a], Moumita Ghosh [b], Subhash C. Bagui [c], Pritha Das [a], Dibakar Ghosh [d], Matjaž Perc [e,f,g,h,*]

[a] Department of Mathematics, Indian Institute of Engineering Science and Technology, Shibpur, Howrah, 711103, India
[b] Department of Mathematics, School of Computer Science and Artificial Intelligence, SR University, Warangal, 506371, India
[c] Department of Mathematics and Statistics, The University of West Florida, Pensacola, FL 32514, USA
[d] Physics and Applied Mathematics Unit, Indian Statistical Institute, 203 B. T. Road, Kolkata, 700108, India
[e] Faculty of Natural Sciences and Mathematics, University of Maribor, Koroška cesta, 160, 2000 Maribor, Slovenia
[f] Community Healthcare Center Dr. Adolf Drolc Maribor, Ulica talcev 9, 2000 Maribor, Slovenia
[g] Department of Physics, Kyung Hee University, 26 Kyungheedae-ro, Dongdaemun-gu, Seoul, 02447, Republic of Korea
[h] University College, Korea University, 145 Anam-ro, Seongbuk-gu, Seoul, 02841, Republic of Korea

ARTICLE INFO

Keywords:
Stochastic dengue model
Basic reproduction number
Sensitivity analysis
Model calibration
Noise-induced extinction
Stochastic optimal control

ABSTRACT

Dengue fever is a mosquito-borne viral disease that continues to pose a substantial public health burden in tropical and subtropical regions. Although most existing studies are based on deterministic formulations, environmental variability and behavioral responses can significantly influence transmission dynamics. In this work, we formulate and analyze a stochastic dengue transmission model that incorporates media-driven awareness, nonlinear treatment responses, and environmental noise. The stochastic system is shown to be well posed by establishing the existence, uniqueness, and positivity of global solutions. The model parameters are estimated by calibrating the deterministic counterpart of the stochastic system against the reported data on dengue incidence, demonstrating good agreement between simulations and observations. The basic reproduction number is derived and sensitivity of the parameters is assessed using partial rank correlation coefficients under uncertainty to identify key drivers of transmission. Analytical conditions for noise-induced disease extinction are obtained, revealing that sufficiently strong environmental fluctuations can suppress endemic persistence. The impact of varying noise intensities on long-term dynamics is further characterized. Finally, we develop a stochastic optimal control framework that integrates awareness-based prevention and treatment interventions, providing a theoretical basis for evaluating control strategies under environmental uncertainty.

1. Introduction

Being a vector borne viral disease, dengue is transmitted primarily by the Aedes aegypti mosquito, caused by four antigenically distinct serotypes of the dengue virus (DENV-1 to DENV-4). According to the WHO, reports indicate record-breaking cases exceeding 7.6 million in 2024, reflecting an alarming eight-fold increase since 2000 [1]. The expansion of the disease is triggered by climate change that extends the habitats of Aedes mosquitoes, rapid urbanization, and the complex interaction of four distinct antigenically and immunologically serotypes that exhibit antibody-dependent enhancement (ADE) - where secondary heterotypic infections often

* Corresponding author at: Faculty of Natural Sciences and Mathematics, University of Maribor, Koroška cesta, 160, 2000 Maribor, Slovenia.
E-mail address: matjaz.perc@gmail.com (M. Perc).

https://doi.org/10.1016/j.amc.2026.130156
Received 31 March 2026; Received in revised form 21 April 2026; Accepted 9 May 2026

lead to severe outcomes [2,3]. The early mathematical models of dengue transmission primarily used classical compartmental frameworks to represent fundamental interactions between human hosts and mosquito vectors [4,5]. Vertical transmission in mosquitoes, which contributes to virus persistence during inter-epidemic periods, has been incorporated to better reflect disease dynamics [6]. Temperature and climate variability have also been shown to significantly influence mosquito breeding, biting rates, and viral replication, prompting models that integrate seasonal or temperature dependent parameters [7–10]. Over the years, researchers have developed various mathematical models to capture the complex dynamics of disease transmission by incorporating multiple biological, environmental, and behavioral factors along with multi strain interactions and optimal intervention strategies [11]. In recent years, evolutionary game theory has emerged as an effective framework for modeling adaptive behavioral responses and strategy evolution in interacting populations, providing deeper insights into cooperation, competition, and resource utilization [12–14]. In parallel, more complex transmission mechanisms have also been explored, including multi-host and intermediate host structures, which can significantly influence disease spread [15]. Some models account for spatial heterogeneity, using metapopulation to simulate local transmission and human mobility between regions [16–18]. More recently, machine learning assisted models have been developed to enhance dengue forecasting and risk mapping by integrating epidemiological and meteorological datasets [19–21]. Behavioral responses to media awareness campaigns, public health interventions, and individual risk perception have been modeled using awareness based incidence rates [22–25]. These effects are particularly pronounced when media campaigns trigger preventive measures such as mosquito avoidance and water storage management. The integration of media dependent contact rates has revealed nonlinear dynamics where awareness saturation can reduce intervention efficacy over time [26]. In addition to media driven prevention, timely and effective treatment also plays a crucial role in managing dengue infections. Nonlinear treatment functions are often introduced in models to capture saturation effects and resource constraints in healthcare systems [27]. In addition, several studies have introduced stochastic formulations to better capture the randomness in environmental and demographic processes that influence transmission. White noise perturbations and Lévy jumps have been employed to model fluctuations in mosquito population, biting rates, and transmission probabilities [28–31]. Studies have demonstrated that such stochastic effects can significantly alter threshold conditions like the basic reproduction number R_0 potentially leading to disease eradication which offers insights into extinction probabilities, outbreak persistence, and noise induced thresholds under noise driven extinction scenarios [32,33]. Recognizing the unpredictability of real world conditions, recent studies have explored stochastic optimal control strategies to mitigate dengue spread and to minimize infection burden and intervention costs by dynamically adjusting control variables in noisy environments [34–37].

Although a substantial body of literature exists on dengue transmission modeling, several important aspects remain insufficiently explored. In particular, models that simultaneously incorporate media induced awareness affecting transmission, nonlinear treatment responses reflecting limited healthcare capacity, and stochastic environmental perturbations are still scarce. Moreover, while optimal control approaches have been widely applied to deterministic dengue models, their extension to stochastic settings especially with rigorous analytical treatment of extinction conditions has received limited attention.

This work presents a comprehensive stochastic modeling framework for dengue transmission that integrates media induced awareness, nonlinear treatment saturation reflecting limited healthcare capacity, and environmental randomness within a single model. In contrast to most existing studies that focus either on deterministic dynamics or purely simulation-based stochastic effects, we derive rigorous analytical conditions for noise induced disease extinction in both human and mosquito populations. The deterministic counterpart of the model is calibrated and validated using real epidemiological data, ensuring biological relevance and providing a reliable baseline for stochastic analysis. Furthermore, a stochastic optimal control framework is formulated to jointly assess awareness-based prevention and treatment strategies under uncertainty, and the corresponding optimality system is solved numerically. This combined analytical data driven and control oriented approach offers new insights into how awareness, stochastic perturbations, and optimal interventions interact to shape dengue transmission dynamics, extending beyond the scope of existing noise-free models.

2. Formulation of the stochastic model

Dengue fever is a vector-borne disease transmitted between humans and mosquitoes, with transmission dynamics strongly influenced by environmental variability, behavioral responses, and intervention effectiveness. While deterministic models describe average epidemic trends, they cannot adequately account for random fluctuations arising from climate variability, heterogeneous contact patterns, and demographic uncertainty. To capture both the biological structure of the disease and the inherent randomness present in real-world transmission, we formulate a stochastic dengue transmission model incorporating random perturbations in the population dynamics. To analyze the disease dynamics, we classify the human population into three compartments: susceptible (S_h), infected (I_h) and recovered (R_h), while the mosquito population is divided only into susceptible (S_m) and infected (I_m). Disease transmission occurs when susceptible humans are bitten by infected mosquitoes and when susceptible mosquitoes acquire infection by biting infected humans. To construct the model, the following assumptions are made:

- The populations are assumed to mix homogeneously, implying that each individual has an equal probability of interaction.
- Susceptible humans are recruited at a constant rate A_h through birth or immigration. Over the short time scale of dengue outbreaks, human demographic changes are assumed negligible, with births and natural deaths approximately balanced.
- Susceptible humans (S_h) become infected when bitten by infected mosquitoes (I_m) at a rate determined by the mosquito biting rate α and the effective transmission rate $\beta_e = \left(\beta - \frac{\beta_1 \eta}{\beta_2 + \eta}\right)$. Here, the baseline transmission rate in the absence of any intervention is given by β, representing the inherent probability of dengue transmission from infected mosquitoes to susceptible humans. This baseline rate is modulated by awareness driven control measures, such as educational campaigns, the use of insecticide-treated nets, repellents, and environmental management, which induce behavioral changes that reduce human exposure to mosquito

bites. The parameter η represents the efficacy level of awareness control. The parameter β_1 represents the maximum achievable reduction in transmission due to awareness, while β_2 is the half-saturation constant, indicating the level of awareness at which half of the maximum reduction is realized. The term $\frac{\beta_1\eta}{\beta_2+\eta}$ thus captures the saturating effect of awareness interventions, where additional efforts yield diminishing returns at higher levels of awareness.

- The treatment rate of infected humans is modeled by the nonlinear function

$$T(I_h) = \frac{aI_h^2}{bI_h^2 + cI_h + 1},$$

which follows a Holling type III functional response. This form captures the limited responsiveness of treatment efforts at low infection levels due to misdiagnosis and underreporting, the rapid mobilization of healthcare resources during moderate outbreaks, and eventual saturation caused by finite medical capacity. The parameter 'a' represents the maximum achievable cure rate due to treatment, with aI_h^2 driving an initial increase in treatment as infection levels rise. However, as I_h grows, the denominator $(bI_h^2 + cI_h + 1)$ dominates, leading to saturation and limiting $T(I_h)$ to an upper bound of $\frac{a}{b}$. The parameter 'b' determines how fast the treatment function saturates due to high levels of infection that represent constraints such as resource depletion and limitations in medical personnel, while the parameter 'c' accounts for baseline inefficiencies in treatment, such as diagnostic delays or pre-existing healthcare burdens, affecting recovery even at lower infection levels. This Holling type III form is particularly relevant for dengue transmission, where treatment availability and efficiency are not proportional to the number of cases. At low infection levels, treatment is often limited due to misdiagnosis, underreporting of mild or asymptomatic cases, and the absence of large scale preparedness, resulting in a weak initial response. As infections increase, health systems mobilize more resources and treatment efforts accelerate disproportionately, consistent with the sigmoidal increase in $T(I_h)$. However, at very high infection burdens, hospitals and healthcare systems reach saturation because of finite beds, medical staff, and diagnostic capacity, which restricts further increases in treatment despite rising cases. Thus, this functional form realistically captures the nonlinear and capacity-limited nature of dengue case management, making it a suitable choice for modeling treatment in this context.
- Infected humans recover naturally at rate r_h or through treatment at rate $T(I_h)$, while disease-induced mortality occurs at rate d. All human compartments experience natural mortality at rate d_h. Recovered individuals acquire immunity and do not participate further in disease transmission.
- The mosquito population follows logistic growth with carrying capacity K, reflecting environmental constraints such as breeding site availability and climatic conditions. Mosquitoes are recruited at rate δ, and transmission from infected humans to susceptible mosquitoes occurs at rate β_m through bites at rate α. Natural mosquito mortality occurs at rate d_m.

Dengue transmission is highly sensitive to random environmental and socio-behavioral factors. Temperature and rainfall fluctuations affect mosquito lifespan, biting frequency, and viral incubation periods, while abrupt environmental changes can alter mosquito population densities. Human mobility, reporting delays, and variability in intervention implementation further introduce uncertainty into disease dynamics. Deterministic models, although useful for capturing average epidemic trends, are unable to represent irregular outbreak timing, sudden epidemic surges, or stochastic disease extinction observed in real data. To account for these uncertainties, we introduce stochastic perturbations into the population dynamics by incorporating multiplicative white noise terms. These perturbations represent both intrinsic biological variability and extrinsic environmental fluctuations. The resulting stochastic dengue transmission model is described by the following system of stochastic differential equations:

$$\begin{aligned}
dS_h &= \left[A_h - \alpha\left(\beta - \frac{\beta_1\eta}{\beta_2+\eta}\right)S_h I_m - d_h S_h\right]dt + \sigma_1 S_h dW_1,\\
dI_h &= \left[\alpha\left(\beta - \frac{\beta_1\eta}{\beta_2+\eta}\right)S_h I_m - r_h I_h - \frac{aI_h^2}{bI_h^2 + cI_h + 1} - dI_h - d_h I_h\right]dt + \sigma_2 I_h dW_2,\\
dR_h &= \left[r_h I_h + \frac{aI_h^2}{bI_h^2 + cI_h + 1} - d_h R_h\right]dt + \sigma_3 R_h dW_3,\\
dS_m &= \left[\delta\left(1 - \frac{S_m + I_m}{K}\right)(S_m + I_m) - \alpha\beta_m S_m I_h - d_m S_m\right]dt + \sigma_4 S_m dW_4,\\
dI_m &= \left[\alpha\beta_m S_m I_h - d_m I_m\right]dt + \sigma_5 I_m dW_5.
\end{aligned} \tag{1}$$

Here, $\{W_i(t)\}_{i=1}^5$ are mutually independent standard Wiener processes defined on a complete probability space $(\Omega, \mathbb{F}, \{\mathbb{F}_t\}_{t\geq 0}, \mathbb{P})$, where the filtration $\{\mathbb{F}_t\}_{t\geq 0}$ satisfies the usual conditions. The parameters σ_i $(i = 1, 2, 3, 4, 5)$ denote the intensities of the stochastic perturbations.

2.1. Existence and uniqueness of global positive solution

Before analyzing the dynamical behavior of the stochastic model (1), we first verify the existence, uniqueness, and positivity of its solutions to ensure that the model is biologically meaningful and mathematically consistent.

Theorem 1. *Given any initial condition* $\left(S_h(0), I_h(0), R_h(0), S_m(0), I_m(0)\right) \in \mathbb{R}^5_+$, *the system (1) admits a unique positive solution for all* $t \geq 0$, *which remains positive in* $\mathbb{R}^5_+$ *with probability one, almost surely (a.s.).*

Proof. Since the coefficients of system (1) are locally Lipschitz continuous, the system admits a unique local positive solution on the interval $[0, \tau_e)$ almost surely, where τ_e denotes the explosion time (see [38]). To establish the global existence of the solution, it suffices to show that $\tau_e = \infty$ almost surely. Let, $n_0 > 0$ be sufficiently large so that $\left(S_h(0), I_h(0), R_h(0), S_m(0), I_m(0)\right) \in \left[\frac{1}{n_0}, n_0\right]$. For each $n \geq n_0$ we define τ_n as

$$\tau_n = inf\left\{t \in [0, \tau_e) : S_h \notin (\tfrac{1}{n}, n) \text{ or } I_h \notin (\tfrac{1}{n}, n) \text{ or } R_h \notin (\tfrac{1}{n}, n) \text{ or } S_m \notin (\tfrac{1}{n}, n) \text{ or } I_m \notin (\tfrac{1}{n}, n)\right\}$$

here, $inf\,\phi$(empty set) $= \infty$. Since τ_n is increasing as $n \to \infty$, we can define $\tau_\infty = \lim_{n\to\infty} \tau_n$ then $0 \leq \tau_\infty \leq \tau_e$. To complete the proof, we need to show that $\tau_\infty = \infty$. If the statement is false, then there exists constants $T > 0$ and $\epsilon \in (0, 1)$ such that $\mathbb{P}(\tau_\infty \leq T) > \epsilon$ for all $n > n_0$.

Define a function $V : \mathbb{R}^5_+ \to \mathbb{R}_+$ as

$$V(S_h, I_h, R_h, S_m, I_m) = (S_h - 1 - \ln S_h) + (I_h - 1 - \ln I_h) + (R_h - 1 - \ln R_h) + (S_m - 1 - \ln S_m) + (I_m - 1 - \ln I_m)$$

Clearly the function V is non-negative in its domain. Using Itô's formula on V we get,

$$\begin{aligned} dV(S_h, I_h, R_h, S_m, I_m) = LV(S_h, I_h, R_h, S_m, I_m)dt + \sigma_1(S_h - 1)dW_1 + \sigma_2(I_h - 1)dW_2 \\ +\sigma_3(R_h - 1)dW_3 + \sigma_4(S_m - 1)dW_4 + \sigma_5(I_m - 1)dW_5 \end{aligned} \tag{2}$$

where the operator LV is a map from $\mathbb{R}^5_+$ into $\mathbb{R}$ defined as

$$\begin{aligned} LV(S_h, I_h, R_h, S_m, I_m) = &\left[\left(1 - \frac{1}{S_h}\right)\left(A_h - \alpha\beta_e S_h I_m - d_h S_h\right) + \left(1 - \frac{1}{I_h}\right)\left(\alpha\beta_e S_h I_m - r_h I_h - \frac{aI_h^2}{bI_h^2 + cI_h + 1} - dI_h - d_h I_h\right)\right. \\ &+ \left(1 - \frac{1}{R_h}\right)\left(r_h I_h + \frac{aI_h^2}{bI_h^2 + cI_h + 1} - d_h R_h\right) \\ &+ \left(1 - \frac{1}{S_m}\right)\left(\delta\left(1 - \frac{S_m + I_m}{K}\right)(S_m + I_m) - \alpha\beta_m S_m I_h - d_m S_m\right) \\ &\left. + \left(1 - \frac{1}{I_m}\right)\left(\alpha\beta_m S_m I_h - d_m I_m\right)\right] + \frac{1}{2}\left[\sigma_1^2 + \sigma_2^2 + \sigma_3^2 + \sigma_4^2 + \sigma_5^2\right] \\ &\leq M \end{aligned}$$

Where,

$$M = A_h + 3d_h + d + r_h + 2d_m + \alpha\beta_e(M_5 + M_1 M_5) + 2a + r_h M_2 + \delta(M_4 + M_5) + \alpha\beta_m M_2(1 + M_4) + \frac{1}{2}\left[\sigma_1^2 + \sigma_2^2 + \sigma_3^2 + \sigma_4^2 + \sigma_5^2\right]$$

with M_1, M_2, M_4, M_5 as the respective supremum of S_h, I_h, S_m, I_m. Then Eq. (1) implies

$$dV(S_h, I_h, R_h, S_m, I_m) = Mdt + \sigma_1(S_h - 1)dW_1 + \sigma_2(I_h - 1)dW_2 + \sigma_3(R_h - 1)dW_3 + \sigma_4(S_m - 1)dW_4 + \sigma_5(I_m - 1)dW_5 \tag{3}$$

Integrating Eq. (3) by Itô's formula from 0 to $t_n = min\{\tau_n, t\} = \tau_n \wedge t$ with $t \leq T$ then taking the expectation we obtain

$$\mathbb{E}V\left(S_h(t_n), I_h(t_n), R_h(t_n), S_m(t_n), I_m(t_n)\right) \leq V\left(S_h(0), I_h(0), R_h(0), S_m(0), I_m(0)\right) + M\mathbb{E}(t_n) \tag{4}$$

Define $\Omega_n = \{\tau_n \leq T\}$ for all $n \geq n_0$, then $\mathbb{P}(\Omega_n) \geq \epsilon$. Consequently for each $\omega \in \Omega_n$, there exists $\left(S_h(t_n \wedge \omega), I_h(t_n \wedge \omega), R_h(t_n \wedge \omega), S_m(t_n \wedge \omega), I_m(t_n \wedge \omega)\right)$ which either equals to n or $\frac{1}{n}$. Then

$$V\left(S_h(t_n \wedge \omega), I_h(t_n \wedge \omega), R_h(t_n \wedge \omega), S_m(t_n \wedge \omega), I_m(t_n \wedge \omega)\right) \geq \left[(n - 1 - \ln n) \wedge (\tfrac{1}{n} - 1 + \ln n)\right].$$

So, from Eq. (4) we get,

$$\begin{aligned} V\left(S_h(0), I_h(0), R_h(0), S_m(0), I_m(0)\right) + MT &\geq \mathbb{E}\left[1_{\Omega_n}(\omega)V\left(S_h(t_n), I_h(t_n), R_h(t_n), S_m(t_n), I_m(t_n)\right)\right] \\ &\geq \mathbb{P}(\Omega_n)\left[(n - 1 - \ln n) \wedge (\tfrac{1}{n} - 1 + \ln n)\right] \\ &\geq \epsilon\left[(n - 1 - \ln n) \wedge (\tfrac{1}{n} - 1 + \ln n)\right] \end{aligned}$$

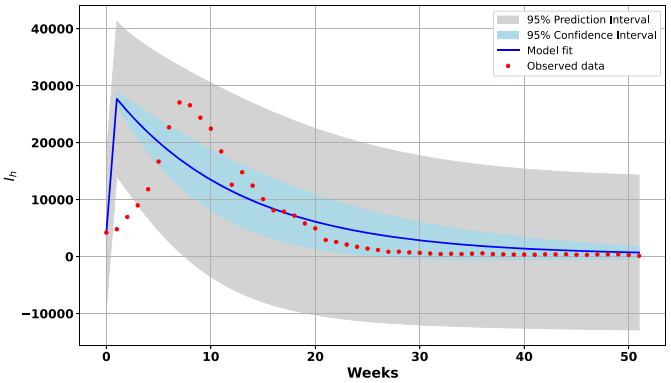

Fig. 1. Deterministic model calibration to weekly dengue incidence data. The blue solid line shows the best-fit solution for $I_h(t)$, red dots indicate reported cases, the light blue band denotes the 95% confidence interval, and the gray band represents the 95% prediction interval.

Table 1
Estimated parameter values obtained from calibration.

Parameter	Estimated Value	Parameter	Estimated Value
A_h	20.14744 ± 0.95322	a	0.49939 ± 0.06475
α	0.20130 ± 0.05587	b	0.50394 ± 0.03275
β	0.05064 ± 0.04139	c	0.30163 ± 0.01538
β_1	0.01020 ± 0.01442	d	0.02299 ± 0.00880
β_2	0.05114 ± 0.05462	δ	0.79392 ± 0.01615
η	0.05027 ± 0.03358	K	9993.98945 ± 983.05945
d_h	0.03609 ± 0.01956	β_m	0.02602 ± 0.01810
r_h	0.01833 ± 0.01622	d_m	0.19014 ± 0.09060

where, $1_{\Omega_n}(\omega)$ is the indicator function of Ω_n. Letting $n \to \infty$ leads to the contradiction as $\infty > V\Big(S_h(0), I_h(0), R_h(0), S_m(0), I_m(0)\Big) + MT = \infty$ which implies $\tau_\infty = \infty$ a.s. and $\tau_e = \infty$. This completes the proof.

□

3. Model validation

Dengue surveillance data summarize transmission processes occurring across large human and mosquito populations and therefore represent mean epidemic behavior. The deterministic model captures these dominant biological mechanisms governing dengue transmission, including average biting rates, recovery rates, and intervention effects, whereas stochastic perturbations describe fluctuations around this mean induced by environmental variability and random contact processes. For this reason, parameter estimation and model validation are carried out using the deterministic system prior to exploring stochastic dynamics.

Setting $\sigma_i = 0$ for all i reduces system (1) to its corresponding deterministic counterpart, which serves as the baseline framework for subsequent analytical and numerical investigations. The deterministic model is validated against weekly dengue incidence data from Rio de Janeiro, Brazil, obtained from the Notifiable Diseases Information System (SINAN) for the year 2024.

The calibration process involves estimating key epidemiological parameters governing human–vector interactions, transmission rates, recovery rates, and natural mortality, such that the model reproduces the observed temporal trends in dengue incidence. Initial conditions for all model compartments are specified using available population data and the reported number of initial infections. Parameter estimation is performed by numerically integrating the deterministic system and applying a nonlinear least-squares optimization based on the Levenberg–Marquardt algorithm to minimize the discrepancy between model predictions and observed dengue cases. The objective function is defined as

$$J(\Theta) = \sum_{i=1}^{n} \left(I_h^{\text{data}}(t_i) - I_h^{\text{model}}(t_i;\Theta) \right)^2,$$

where $I_h^{\text{data}}(t_i)$ and $I_h^{\text{model}}(t_i;\Theta)$ denote the observed and simulated numbers of infected humans at time t_i, respectively, and Θ represents the vector of parameters to be estimated.

The resulting calibrated model successfully reproduces the temporal evolution of dengue cases in Brazil (Fig. 1), demonstrating that the deterministic model captures the key features of disease transmission under realistic conditions. The estimated parameters along with their standard errors (obtained from the covariance matrix) are summarized in Table 1. All parameters are constrained to biologically plausible ranges, ensuring meaningful values for transmission, recovery, and mortality rates. Uncertainty in model predictions is quantified using 95% confidence intervals computed via the delta method, based on the covariance of the estimated

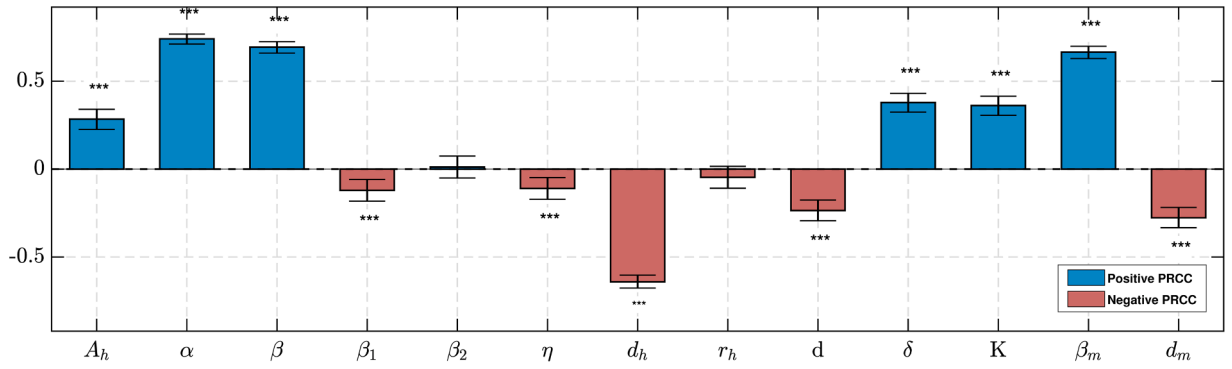

Fig. 2. Sensitivity of R_0 to system parameters based on PRCC analysis. Error bars represent 95% confidence intervals, with (***) denoting parameters whose PRCC values are significant at the $p < .01$ level.

parameters. Additionally, 95% prediction intervals are constructed by incorporating observational variance, accounting for data noise. The fitted parameters reflect region-specific epidemiological, environmental, and demographic factors, indicating that the model effectively captures dengue transmission dynamics despite minor discrepancies due to unmodeled factors such as changes in control measures, climate variability, and reporting differences. This suggests that key epidemiological processes are well represented, supporting the model's reliability for understanding disease spread and guiding prediction and control strategies.

3.1. Sensitivity analysis of R_0

While the calibration results demonstrate that the deterministic model is capable of reproducing the observed dengue incidence, the available data are limited in both temporal span and resolution. Consequently, not all parameters are equally well identified, and several estimates exhibit relatively wide confidence intervals. In such circumstances, it is essential to assess how parameter uncertainty influences key epidemiological quantities. To this end, we conduct a global sensitivity analysis of the basic reproduction number (R_0), whose derivation is provided in Appendix A, using partial rank correlation coefficients (PRCC). This analysis enables the identification of the most influential parameters governing dengue transmission and distinguishes those that strongly affect disease persistence from parameters with weaker impact. The PRCC results thus provide guidance for interpreting the calibrated parameters, prioritizing control-relevant mechanisms, and selecting representative baseline parameter values for subsequent stochastic simulations and optimal control analysis.

The PRCC analysis (Fig. 2) demonstrates that parameters A_h, α, β, δ, K and β_m are strongly and positively correlated with R_0, indicating their disease enhancing effects in dengue transmission. Specifically, higher human recruitment (A_h) increases the pool of susceptible hosts, while increased biting activity (α) and transmission probabilities from humans to mosquitoes (β) and mosquitoes to humans (β_m) intensify virus spread. Similarly, larger mosquito maturation rates (δ) and carrying capacity (K) promote vector abundance, thereby elevating transmission potential. In contrast, the parameters η, d_h, β_1, d_m show significant negative correlations, reflecting their suppressive effects on dengue dynamics. An increase in mosquito mortality (d_m) reduces the lifespan and abundance of infectious vectors, thereby limiting virus transmission, while higher human natural mortality (d_h) and disease induced mortality (d) decrease the effective infectious host population. Importantly, the parameter (η) which quantifies the efficacy of public health awareness interventions, plays a critical role in reducing transmission by modulating the baseline transmission rate (β). Awareness driven measures such as educational campaigns, the use of insecticide treated nets, repellents, and environmental management induce behavioral changes that lower human-mosquito contact, thereby diminishing the effective transmission probability and contributing to a reduction in R_0. Confidence intervals (95%) and p-values are computed to assess the significance of each correlation.

- **Baseline parameter set for numerical simulations:** To ensure consistency across all numerical investigations, a single baseline parameter set, denoted as **Set A**:= $\{A_h = 20,\ \alpha = 0.19,\ \beta = 0.025,\ \beta_1 = 0.025,\ \beta_2 = 0.025,\ \eta = 0.05,\ d_h = 0.1,\ r_h = 0.0254,\ a = 0.5,\ b = 0.5,\ c = 0.3,\ d = 0.0269,\ K = 25,\ \delta = 0.79,\ \beta_m = 0.01,\ d_m = 0.019\}$ is employed for all simulations presented in the subsequent sections selected within the estimated uncertainty ranges obtained from model calibration (Table 1). However, due to the limited temporal span and resolution of the available data, not all parameters are practically identifiable, and some exhibit wide confidence intervals or weak sensitivity during the fitting procedure. For this some of the parameters in **Set A** lies within the estimated ranges reported in Table 1, the remaining parameters are fixed at biologically reasonable values guided by epidemiological considerations and existing literature.

4. Stochastic dynamics near deterministic equilibria

This section analyzes the local stochastic behavior of the dengue transmission model in neighborhoods of the deterministic disease-free equilibrium and endemic equilibrium. Throughout this section, these equilibria refer to those of the deterministic subsystem obtained by setting $\sigma_i = 0$ in system (1). The disease-free equilibrium and the associated basic reproduction number R_0 are derived

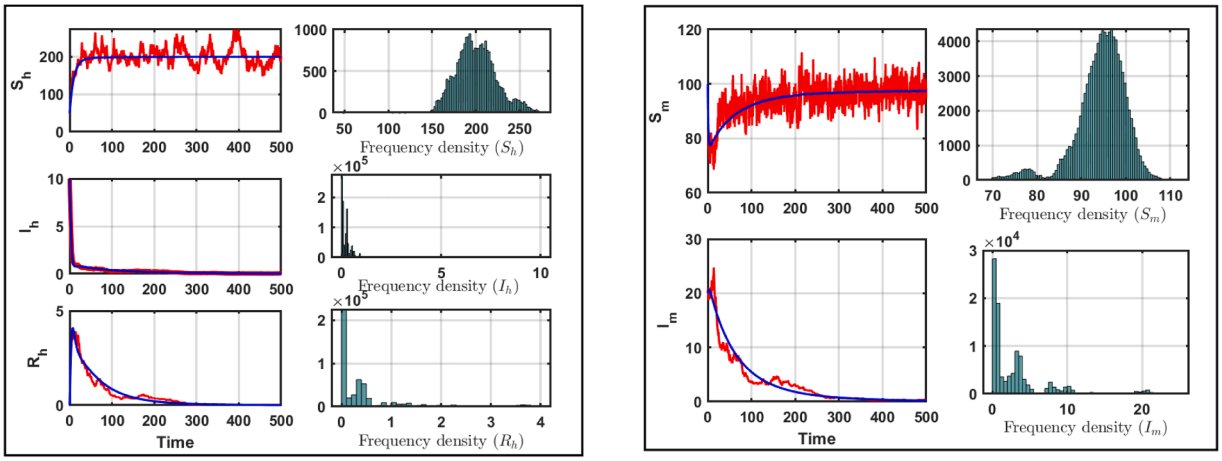

Fig. 3. Time series trajectories of the deterministic model (blue curves) and the corresponding stochastic model (red sample paths) for (a) the human population and (b) the mosquito population. The associated relative frequency density distributions of the stochastic solutions, illustrating convergence and fluctuation around the disease-free equilibrium. These numerical simulations confirm the theoretical result that the disease-free equilibrium is asymptotically stable when $R_0 < 1$, while stochastic perturbations induce bounded oscillations around the equilibrium state.

in Appendix A, while the endemic equilibrium is obtained in Appendix B. The objective of this section is to examine how stochastic perturbations influence the stability and persistence of these equilibria and to assess the robustness of deterministic predictions in the presence of environmental and demographic noise. By linearizing the stochastic system around the disease-free and endemic equilibria, we characterize noise-induced deviations from deterministic trajectories and identify conditions under which stochastic effects may alter disease outcomes.

Theorem 2. *If $R_0 < 1$, then for any initial condition $\left(S_h(0),\ I_h(0),\ R_h(0),\ S_m(0),\ I_m(0)\right) \in \mathbb{R}^5_+$, the solution of the system (1) satisfies the following property*

$$\lim_{t\to\infty} \mathbf{Sup} \frac{1}{t}\mathbb{E}\int_0^t \left[d_h\left(S_h - S_h^0\right)^2 + d_m\left(d + d_h + r_h\right)\left(1 - R_0^2\right)I_h + d_h R_h + d_m\left(S_m - S_m^0\right)^2 + d_m I_m\right]$$
$$\leq \frac{A_h}{d_h}\left(A_h + \alpha\beta_e K\left(S_h^0 + 1\right) + r_h + \alpha\beta_m K\left(S_m^0 + 1\right)\right) + \frac{1}{2}\left(\frac{A_h^2\sigma_1^2}{d_h^2} + \sigma_4^2 K^2 + 2\delta K^2\right)$$

Proof. See Appendix C. □

Theorem 3. *For any initial state $\left(S_h(0),\ I_h(0),\ R_h(0),\ S_m(0),\ I_m(0)\right) \in \mathbb{R}^5_+$, if $R_0 > 1$ and $d_h > \frac{1}{2}\max\{\sigma_1^2, \sigma_2^2, \sigma_3^2\}$, then the solution of system (1) satisfies the following property*

$$\lim_{t\to\infty} \mathbf{Sup} \frac{1}{t}\mathbb{E}\int_0^t \left[d_h\left(S_h - S_h^*\right)^2 + (d + d_h)\left(I_h - I_h^*\right)^2 + d_h\left(R_h - R_h^*\right)^2 + \frac{\delta S_m^*}{\left(S_m^* + I_m^*\right)}\left(\left(S_m - S_m^*\right)^2 + \left(I_m - I_m^*\right)^2\right)\right]$$
$$\leq \frac{A_h}{d_h}(2d_h + d)(S_h^* + 2I_h^* + R_h^*) + 2A_h(R_h^* + S_h^*) + \frac{1}{2d_m}S_m^* K\delta^2 + \frac{A_h^2}{2d_h^2}(\sigma_1^2 + \sigma_2^2 + \sigma_3^2) + \frac{K^2}{2}(\sigma_4^2 + \sigma_5^2)$$

Proof. See Appendix D. □

In order to examine the asymptotic behavior of the proposed model under different transmission regimes, numerical simulations are carried out for both the deterministic system and its stochastic counterpart.

For the case $R_0 = 0.8563 < 1$, the parameter values are chosen as $\{\alpha = 0.1,\ \eta = 0.55,\ K = 100\}$, while all remaining parameters are fixed as in **Set A**, with noise intensities $\{\sigma_1 = \sigma_2 = \sigma_3 = \sigma_4 = \sigma_5 = 0.05\}$. As shown in Fig. 3, all infectious compartments converge to the disease-free equilibrium. The deterministic solution exhibits a monotone decay to zero, confirming the global stability of the disease-free state. In the corresponding stochastic system, the sample paths initially experience random fluctuations induced by environmental noise; however, these fluctuations gradually vanish over time. Consequently, both the infected human and infected mosquito populations (I_h and I_m) approach extinction almost surely, demonstrating that the disease-free equilibrium remains robust under stochastic perturbations.

For the case $R_0 = 3.7908 > 1$, the parameters are adjusted to $\{\alpha = 0.14,\ \eta = 0.55,\ K = 1000\}$, while all remaining parameters are fixed at their baseline values given in **Set A**. The numerical simulations in Fig. 4 show that the deterministic system converges

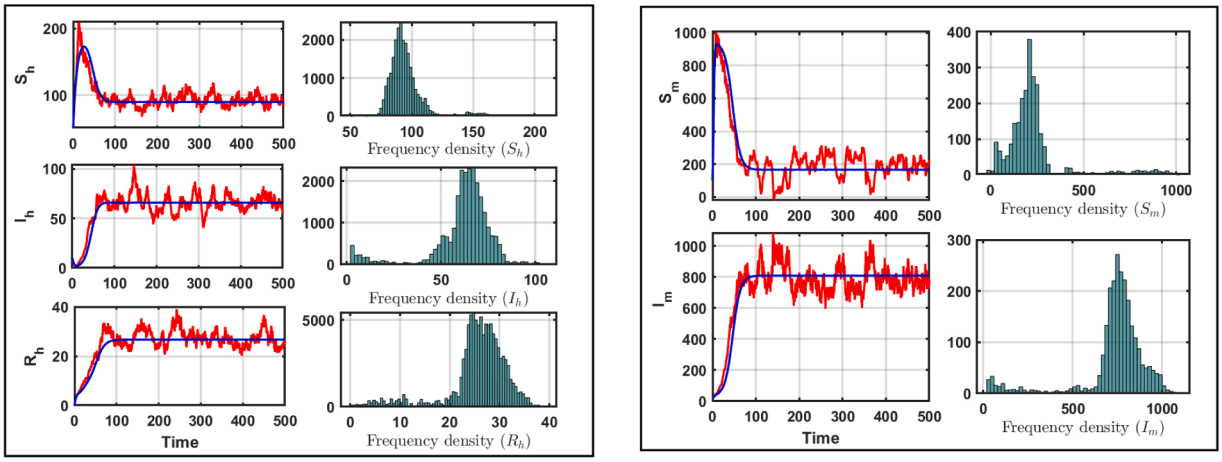

Fig. 4. Time evolution of the deterministic model (blue curves) and the corresponding stochastic model (red curves) for (a) the human population and (b) the mosquito population. The deterministic trajectories converge to a positive endemic equilibrium, while the stochastic solutions exhibit persistent bounded fluctuations around this equilibrium due to environmental noise. The accompanying relative frequency density plots illustrate that the stochastic distributions are centered around the endemic equilibrium level, confirming long-term disease persistence under the condition $R_0 > 1$.

to a positive endemic equilibrium, indicating sustained disease transmission. When the conditions of Theorem (3) are satisfied with equal noise intensities $\sigma_1 = \sigma_2 = \sigma_3 = \sigma_4 = \sigma_5 = 0.05$, the corresponding stochastic trajectories remain stochastically stable around this endemic equilibrium. In particular, the sample paths exhibit persistent bounded fluctuations without converging to zero, confirming long-term infection persistence in the presence of moderate environmental perturbations.

The associated relative frequency density plots further support these observations. For $R_0 < 1$, the relative frequency density plots show that the infected compartments are sharply concentrated near zero, while the remaining state variables are concentrated around their disease-free equilibrium values. This indicates a high probability of disease extinction in both host and vector populations. Conversely, for $R_0 > 1$, the densities are centered around the endemic equilibrium level, demonstrating sustained infection with bounded stochastic variability. These numerical findings are fully consistent with the analytical stability and extinction results derived in this sections.

5. Extinction of disease

To determine the conditions for disease extinction, we analyze the system's stochastic dynamics and identify thresholds where infection dies out.

Theorem 4. *Let* $\left(S_h,\ I_h,\ R_h,\ S_m,\ I_m\right)$ *be the solution of the system (1) with the initial condition* $\left(S_h(0),\ I_h(0), R_h(0),\ S_m(0),\ I_m(0)\right) \in \mathbb{R}^5_+$. *If either condition 1 or 2 holds:*

1. $R_0^m = \dfrac{\delta\,(d + d_h + r_h)\,R_0^2}{\alpha\left(\beta - \frac{\beta_1 \eta}{\beta_2 + \eta}\right)(\delta - d_m)} - \dfrac{\sigma_5^2}{2d_m} < 1,$
2. $R_0^h = \dfrac{\delta\, d_m\, R_0^2}{\alpha\beta_m(\delta - d_m)} - \dfrac{\sigma_2^2}{2(d + d_h + r_h)} - \dfrac{a}{\left(2\sqrt{b} + c\right)(d + d_h + r_h)} < 1,$

then the disease will go extinct in both host and vector populations, i.e., $\lim_{t\to\infty} I_h(t) = 0$ *and* $\lim_{t\to\infty} I_m(t) = 0$ *exponentially with probability one.*

Proof. See Appendix E. □

To numerically validate the theoretical conditions for disease extinction, we conduct 100 Monte Carlo simulations of the stochastic dengue transmission model. The simulations are performed using the parameter values $\{\alpha = 0.14,\ \eta = 0.55,\ a = 0.6,\ b = 0.2,\ c = 0.2,\ \beta_m = 0.001,\ d_m = 0.6\}$, while all remaining parameters are fixed according to **Set A.** The stochastic perturbations are introduced through the noise intensities $\sigma_1 = 0.05,\ \sigma_2 = 0.5,\ \sigma_3 = 0.05,\ \sigma_4 = 0.05,\ \sigma_5 = 0.5$. Simulations are initialized at $\left(S_h(0),\ I_h(0),\ R_h(0),\ S_m(0),\ I_m(0)\right) = \left(500,\ 100,\ 0,\ 1000,\ 200\right)$. As illustrated in Fig. 5, the infected human (I_h) and infected mosquito (I_m) populations exhibited extinction (defined as $I_h < 10^{-5}$ and $I_h < 10^{-5}$, respectively). this reflects a situation in which sustained human-mosquito transmission chains can no longer be maintained, effectively leading to the interruption of dengue spread.

The histograms and box plots further quantify the variability in extinction times across stochastic realizations, capturing the inherent randomness in dengue transmission due to fluctuating environmental conditions and mosquito dynamics. The mean extinction time for infected humans was estimated as (49.96 ± 11.44) time units, while infected mosquitoes exhibited a shorter mean extinction time of for (24.69 ± 3.54) time units. The faster extinction of infected mosquitoes reflects their shorter lifespan and higher sensitivity to environmental variability, which directly limits their ability to sustain viral transmission to humans. Together, these results highlight the critical role of vector population dynamics in driving dengue extinction under stochastic perturbations. These results align with the conditions of Theorem (4) as $R_0^h = 0.5754 < 1$ and $R_0^m = 0.9583 < 1$. This result confirms that when the average number of secondary infections generated by both infected humans and infected mosquitoes falls below unity, dengue transmission cannot persist, even in the presence of environmental noise.

Overall, the analytical and numerical results consistently show that maintaining either of the reproduction thresholds below unity ensures disease extinction. These findings highlight the crucial role of transmission reduction in both human and vector populations for achieving effective disease control. The shorter extinction time of infected mosquitoes further indicates their higher sensitivity to environmental variability, suggesting that targeting vector dynamics can significantly accelerate disease elimination.

6. Effect of noise intensities on stochastic system

To investigate the influence of environmental fluctuations on dengue disease transmission, numerical simulations of the system (1) are performed using the parameter set $\{\eta = 0.55,\ a = 0.6,\ b = 0.2,\ c = 0.1,\ d = 0.269,\ \beta_m = 0.2\}$, while all remaining parameters are fixed according to **Set A**. For this parameter regime, the basic reproduction number is calculated as $R_0 = 2.261 > 1$, indicating that, in the absence of stochastic perturbations, the disease persists in the population.

To assess the impact of stochastic effects, the noise intensities are varied uniformly across all stochastic components, i.e., $\sigma = \sigma_1 = \sigma_2 = \sigma_3 = \sigma_4 = \sigma_5$. The same initial conditions, $\Big(S_h(0),\ I_h(0),\ R_h(0),\ S_m(0),\ I_m(0)\Big) = (20,\ 5,\ 0,\ 50,\ 10)$ and identical parameter values are used for both the deterministic and stochastic simulations to ensure a consistent and meaningful comparison. As shown in Fig. 6(a), for small noise intensities ($\sigma = 0.01$), the stochastic trajectories closely follow the deterministic solution, maintaining oscillations characteristic of endemic infection and introduces variability in the trajectory, but the disease still persists as $R_0^h = 1.088 > 1$. At higher noise levels ($\sigma = 0.9$) shown in Fig. 6(c), the infected human and infected mosquito populations decline steadily and eventually reach extinction, although $R_0 > 1$. In particular, larger noise intensities lead to faster extinction times. These results suggest that environmental noise can destabilize disease persistence and lead to extinction of infection in both host and vector populations.

To further quantify this phenomenon, we focus on host-specific stochastic perturbations, motivated by the extinction condition derived in Theorem (4), where the threshold R_0^h explicitly depends on the noise intensity σ_2 associated with the infected human population. Fixing all other noise terms and varying σ_2, we compute the extinction probability of I_h across a range of values of σ_2 and R_0^h. The resulting contour plot in Fig. 6(b) demonstrates that increasing stochastic fluctuations in the infected host class substantially increases the probability of disease extinction. In particular, for sufficiently large σ_2, extinction occurs with high probability, despite the deterministic system predicts endemic persistence with $R_0 = 2.261 > 1$.

These results demonstrate that environmental noise fundamentally alters dengue transmission dynamics. In particular, when all noise intensities are set to zero ($\sigma_i = 0$), the deterministic model predicts sustained infection due to $R_0 = 2.261 > 1$, whereas the introduction of stochastic perturbations alone can drive the disease to extinction. This highlights the critical role of randomness in realistic epidemic settings and underscores the necessity of incorporating stochastic effects when designing intervention strategies. Consequently, these findings provide strong motivation for the stochastic optimal control framework developed in the subsequent section.

7. Optimization by awareness for prevention control and treatment control emphasizing maximum cure rate of infected individuals

Considering the severity and unpredictability of dengue outbreaks, an optimal control model is formulated by rewriting system (1) and solving it under stochastic perturbations. In realistic epidemiological settings, disease transmission is influenced by random environmental fluctuations, climatic variability, vector population changes, and behavioral uncertainties. Deterministic control strategies may fail to capture these uncertainties, potentially leading to suboptimal or unstable intervention policies.

Therefore, the objective of this section is to develop a *stochastic optimal control framework* that determines robust and cost-effective intervention strategies in the presence of random external disturbances. The purpose of incorporating stochastic optimal control is:

- to design prevention and treatment strategies that remain effective under environmental and demographic randomness,
- to minimize the expected number of infected individuals over a given time horizon,
- to maximize the cure rate of infected individuals through enhanced medical efforts,
- and to minimize the overall implementation cost of awareness and treatment controls.

Two control strategies are considered as follows:

(i) Awareness for prevention control $u_1(t)$ that encourages individuals to adopt preventive measures against dengue. In this section, the transmission-related parameter η is replaced by the control variable $u_1(t)$, and its impact on curbing disease spread is analyzed. The control $u_1(t)$ quantifies the efforts of awareness campaigns for dengue prevention, including the use of mosquito nets, sanitation of

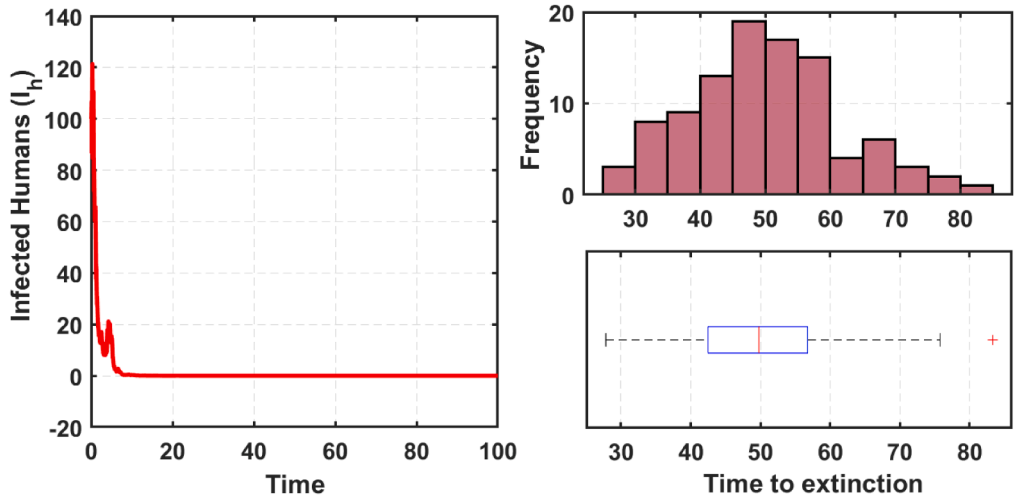

(a)

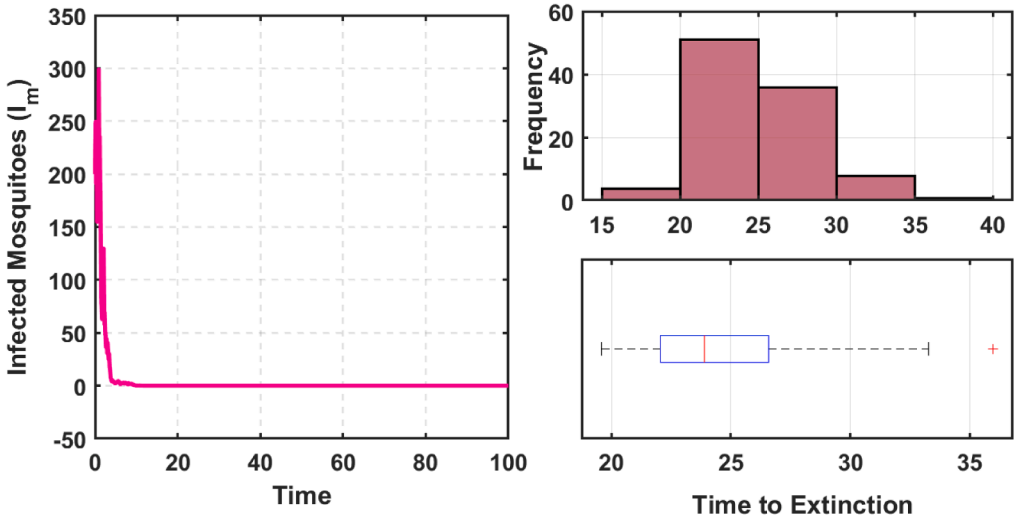

(b)

Fig. 5. Stochastic extinction dynamics of dengue infection in humans and mosquitoes. (a) Time series of infected humans (I_h), illustrating stochastic extinction for $R_0^h = 0.5754 < 1$, with the associated histogram and box plot of extinction times obtained from 100 Monte Carlo simulations, highlighting the variability in the time required for the elimination of human dengue infections due to environmental and demographic fluctuations. (b) Time series of infected mosquitoes (I_m) showing stochastic extinction for $R_0^m = 0.9583 < 1$, together with the corresponding extinction-time distributions, indicating faster extinction in the vector population under stochastic perturbations.

local areas, and other health education measures. Since awareness campaigns target the entire human population, the associated cost is proportional to the total human population, and the cost of u_1 is taken as $u_1(t)(S_h + I_h + R_h)$.

(ii) Treatment control $u_2(t)$ that emphasizes maximizing the cure rate. Here, the cure rate parameter a in (1) is replaced by the control variable $u_2(t)$. The control $u_2(t)$ represents medical efforts including vaccination, medication, hospitalization, and other therapeutic interventions aimed at increasing recovery and reducing the infectious period.

The above mentioned awareness strategy has been seen to be effective in raising social education [39,40].

Incorporating the above control strategies together with random environmental fluctuations in the population growth terms, system (1) is reformulated as the following stochastic controlled system with initial conditions $S_h(0) \geq 0$, $I_h(0) \geq 0$, $R_h(0) \geq 0$, $S_m(0) \geq 0$, and $I_m(0) \geq 0$:

$$ds(t) = F(u(t), s(t))\,dt + G(s(t))\,dW(t), \tag{5}$$

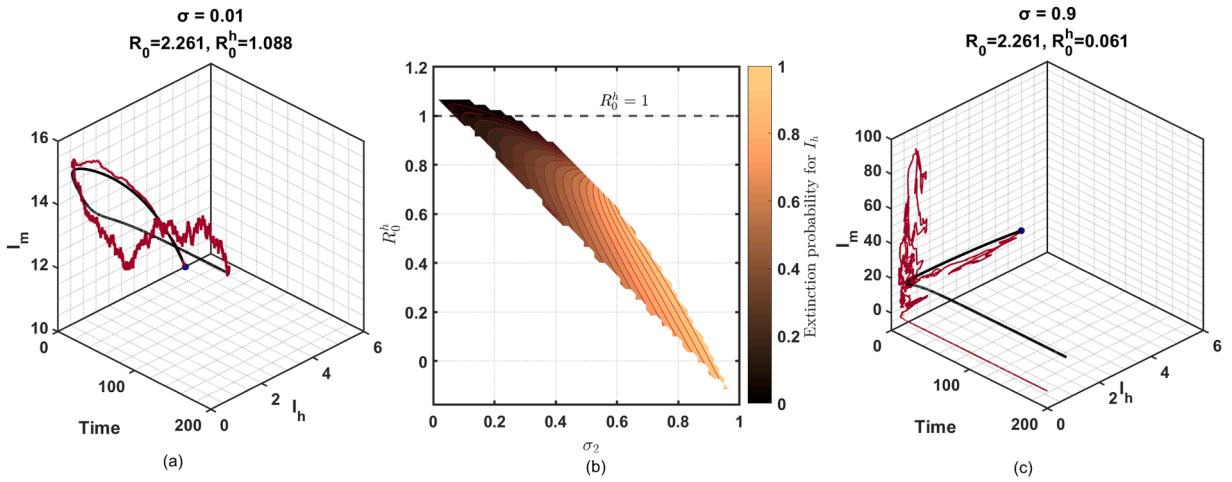

Fig. 6. Extinction probability of infected humans I_h in the $(\sigma_2,\ R_0^h)$-plane. The dashed line indicates $R_0^h = 1$.

where the drift components are given by

$$
\begin{aligned}
f_1 &= A_h - \alpha\left(\beta - \frac{\beta_1 u_1}{\beta_2 + u_1}\right) S_h I_m - d_h S_h,\\
f_2 &= \alpha\left(\beta - \frac{\beta_1 u_1}{\beta_2 + u_1}\right) S_h I_m - r_h I_h - \frac{u_2 I_h^2}{b I_h^2 + c I_h + 1} - d I_h - d_h I_h,\\
f_3 &= r_h I_h + \frac{u_2 I_h^2}{b I_h^2 + c I_h + 1} - d_h R_h,\\
f_4 &= \delta\left(1 - \frac{S_m + I_m}{K}\right)(S_m + I_m) - \alpha\beta_m S_m I_h - d_m S_m,\\
f_5 &= \alpha\beta_m S_m I_h - d_m I_m.
\end{aligned}
\tag{6}
$$

The diffusion terms are defined as $g_1 = \sigma_1 S_h,\ g_2 = \sigma_2 I_h,\ g_3 = \sigma_3 R_h,\ g_4 = \sigma_4 S_m,$ and $g_5 = \sigma_5 I_m$, with $u(t) = \left[u_1(t),\ u_2(t)\right]^T$ and $s(t) = \left[S_h(t),\ I_h(t),\ R_h(t),\ S_m(t),\ I_m(t)\right]^T$.

The cost functional is proposed as $c\left(S_h, I_h, R_h, S_m, I_m, u_1, u_2\right) = \left(A_0 I_h + B_0 u_1^2 (S_h + I_h + R_h) + B_1 u_2^2\right)$ which is clearly continuously differentiable. A_0, B_0, and B_1 are positive constants. If $[0, t_f]$ is the duration of executing controls, the cost function is defined as following,

$$
\mathcal{I}(u, s) = \frac{1}{2}\int_0^{t_f} \left(A_0 I_h + B_0 u_1^2 (S_h + I_h + R_h) + B_1 u_2^2\right) dt \tag{7}
$$

Therefore, our objective is to find the optimal strategies $u^*(t) = (u_1^*(t), u_2^*(t))$ such that $\mathcal{I}(u^*, s^*) \le \mathcal{I}(u, s), \forall u \in \Theta$, where Θ is the set of all admissible controls defined as follows:

$$
\Theta = \left\{(u_1, u_2) : u_i \in [0, 1], \forall u_i \in L^2, t \in [0, t_f]\right\}.
$$

Before applying the stochastic maximal principle, we construct the Hamiltonian of the system as follows,

$$
H\left(S_h, I_h, R_h, S_m, I_m, u_1, u_2\right) = A_0 I_h + B_0 u_1^2 (S_h + I_h + R_h) + B_1 u_2^2 + e_1 f_1 + e_2 f_2 + e_3 f_3 + e_4 f_4 + e_5 f_5 + \left\langle g(x), q\right\rangle. \tag{8}
$$

Here, $e = (e_1, e_2, e_3, e_4, e_5)$ and $q = (q_1, q_2, q_3, q_4, q_5)$ are corresponding co-state variables. From the stochastic maximal principle it follows that

$$
de(t) = -\frac{\partial H}{\partial s} dt + q\left(s^*(t)\right) dW(t), \tag{9}
$$

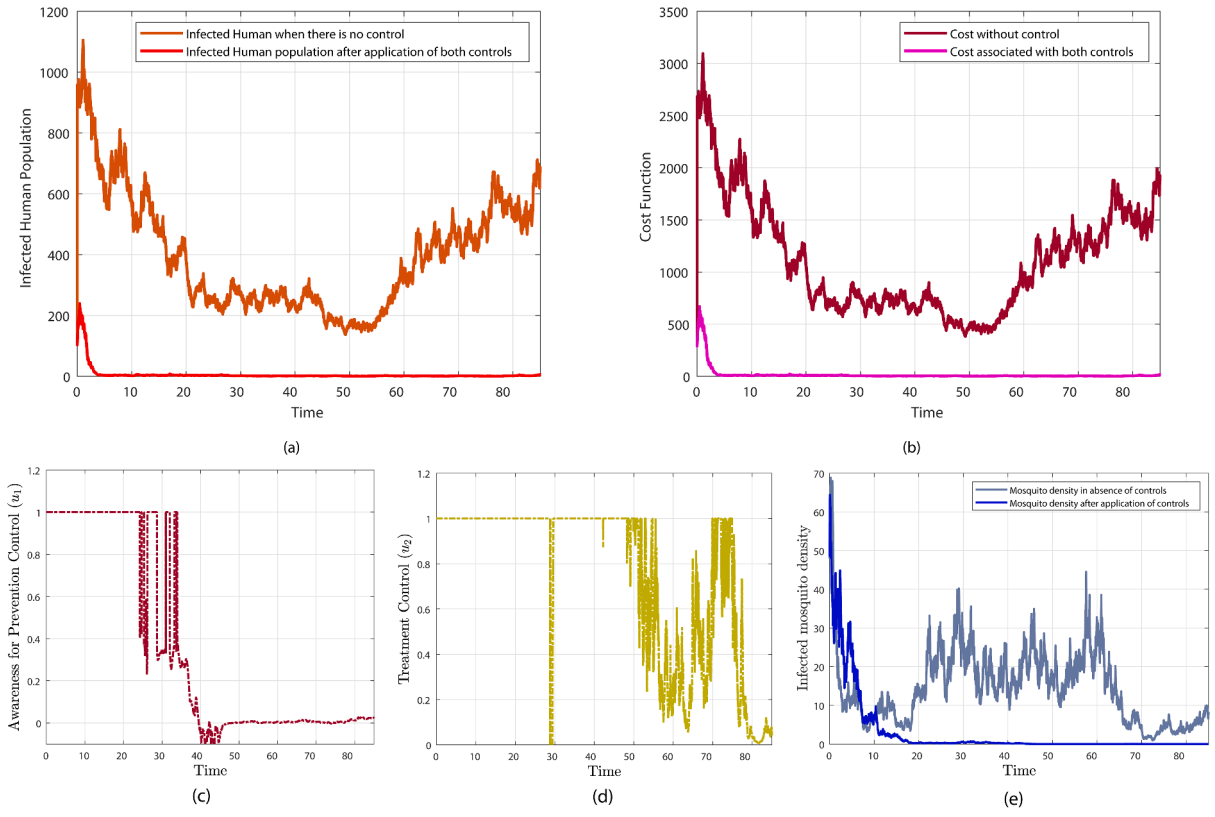

Fig. 7. Impact of optimization on infected population along with the associated cost when both the controls are applied under stochastic environment. (a) Infected human population reduces to a minimum size after application of controls, (b) The associated cost reduces notably in presence of controls, (c) Evolution of Awareness for prevention control with time when both controls are active, (d) Evolution of treatment control with time when both controls are active, and (e) Mosquito density almost extincts after application of controls.

i.e.,

$$
\begin{aligned}
\dot{e}_1 &= -\frac{\partial H}{\partial S_h} = -B_0 {u_1}^2 + e_1\alpha\left(\beta - \frac{\beta_1 u_1}{\beta_2 + u_1}\right) I_m + e_1 d_h - e_2\alpha\left(\beta - \frac{\beta_1 u_1}{\beta_2 + u_1}\right) I_m - \sigma_1 q_1,\\
\dot{e}_2 &= -\frac{\partial H}{\partial I_h} = -A_0 - B_0 {u_1}^2 + r_h(e_2 - e_3) + u_2(e_2 - e_3)\left(\frac{2I_h + c{I_h}^2}{\left(b{I_h}^2 + cI_h + 1\right)^2}\right) + e_2(d + d_h) + (e_4 - e_5)\alpha\beta_m S_m - \sigma_2 q_2,\\
\dot{e}_3 &= -\frac{\partial H}{\partial R_h} = -B_0 {u_1}^2 + e_3 d_h - \sigma_3 q_3,\\
\dot{e}_4 &= -\frac{\partial H}{\partial S_m} = -e_4\delta\left(1 - \frac{2S_m + 2I_m}{K}\right) + e_4\alpha\beta_m I_h + e_4 d_m - e_5\alpha\beta_m I_h - \sigma_4 q_4,\\
\dot{e}_5 &= -\frac{\partial H}{\partial I_m} = e_1\alpha\left(\beta - \frac{\beta_1 u_1}{\beta_2 + u_1}\right) S_h - e_2\alpha\left(\beta - \frac{\beta_1 u_1}{\beta_2 + u_1}\right) S_h - e_4\delta\left(1 - \frac{2S_m + 2I_m}{K}\right) + e_5 d_m - \sigma_5 q_5.
\end{aligned}
\tag{10}
$$

with transversality condition $e_i(t_f) = 0$ for $i = 1, 2, 3, 4, 5$ and $q_i(s)$ are co-state variables for corresponding stochastic system. Now, by the stochastic maximal principle, the optimal control problem is given by

$$
\begin{aligned}
&H(s^*, u^*, e, q) = \max_{u \in \Theta} H(s^*, u, e, q)\\
&\text{Subject to:}\\
&\quad ds(t) = \frac{\partial H}{\partial e}\, dt + G\left(s^*(t)\right) dW(t)\\
&\quad de(t) = -\frac{\partial H}{\partial s}\, dt + q(t)\, dW(t)
\end{aligned}
\tag{11}
$$

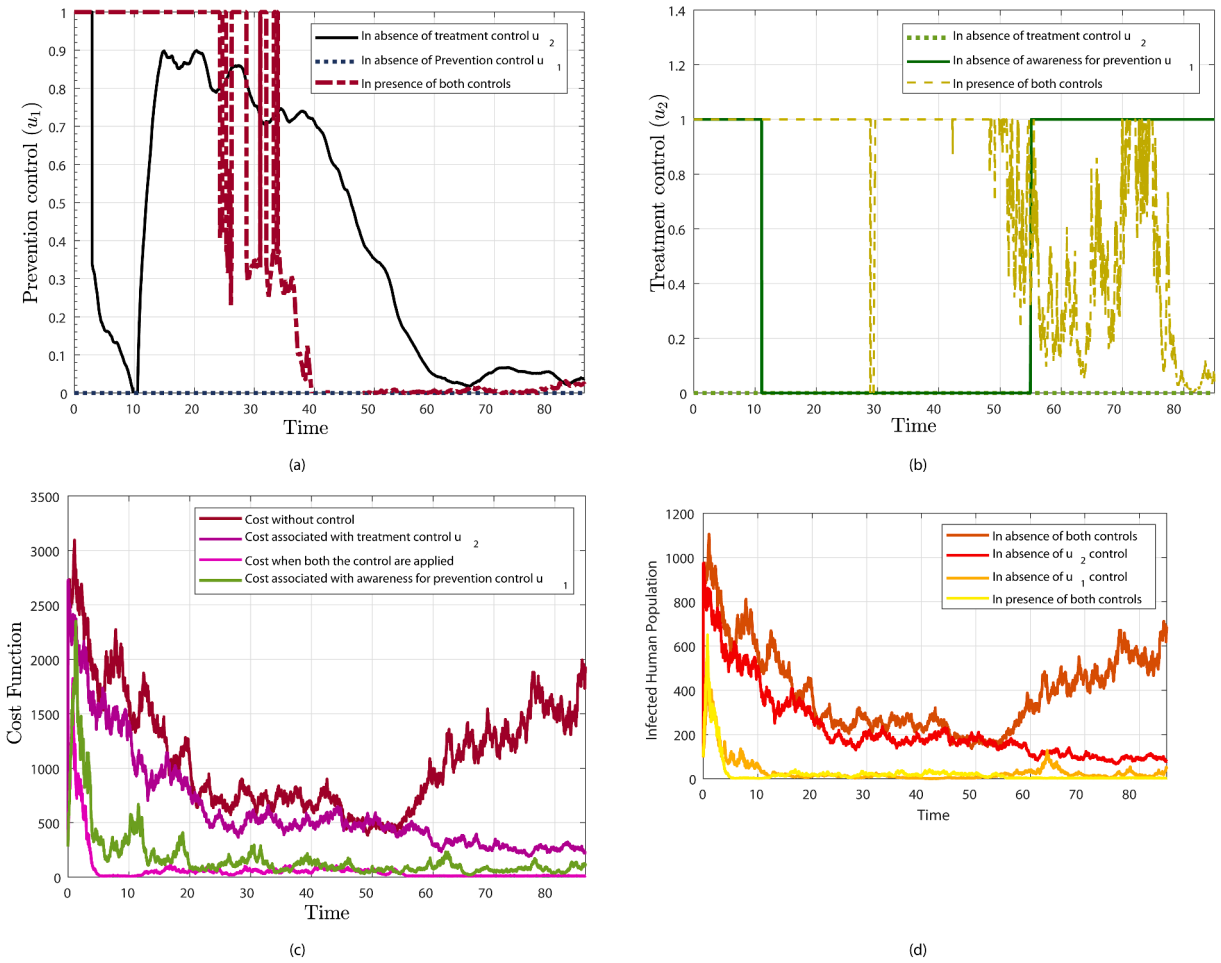

Fig. 8. Simulations show the evolution of controls in various scenarios that also signify the application of controls. (a) Evolution of u_1 control in different scenarios, (b) Evolution of u_2 control in different scenarios, (c) Evolution of cost associated with controls in different scenarios and (d) Evolution of Infected human population size with time in different scenarios.

Now, solving the optimality condition $\frac{\partial H}{\partial u_i} = 0,\ i = 1, 2$ we obtain,

$$u_1^* = \min\left\{\max\left\{\left(\frac{\beta_2{}^3}{27} + \frac{C_4}{2} + \sqrt{\frac{\beta_2{}^3 C_4}{27} + \frac{C_4^2}{4}}\right)^{\frac{1}{3}} + \left(\frac{\beta_2{}^3}{27} + \frac{C_4}{2} - \sqrt{\frac{\beta_2{}^3 C_4}{27} + \frac{C_4^2}{4}}\right)^{\frac{1}{3}} - \frac{2\beta_2}{3}, 0\right\}, 1\right\} \tag{12}$$

where, $C_4 = \dfrac{\alpha\beta_1\beta_2(e_2 - e_1)}{2B_0(S_h + I_h + R_h)}$ and

$$u_2^* = \min\left\{\max\left\{\frac{(e_2 - e_3)I_h{}^2}{2B_1(bI_h{}^2 + cI_h + 1)}, 0\right\}, 1\right\}. \tag{13}$$

7.1. Simulations for stochastic optimal control

To validate the analytical results obtained for the proposed control strategies, numerical simulations are presented in this subsection. The stochastic optimal control problem (11) is solved numerically using MATLAB by means of Monte Carlo simulations combined with the forward-backward sweep method. The number of Monte Carlo iterations is fixed at $N = 10000$. The control measures are implemented over a finite time horizon $t_f = 85$ units of time (may be counted in days). For simulations we have considered following parameter values $\{A_h = 10,\ \eta = 0.55,\ a = 0.6,\ b = 0.2,\ c = 0.1,\ d = 0.269,\ \delta = 0.79,\ \beta_m = 0.2\}$, while all remaining parameters are fixed according to Set A. The corresponding noise intensities are chosen as $\Sigma_1 = \{\sigma_1 = 0.23,\ \sigma_2 = 0.43,\ \sigma_3 = 0.23,\ \sigma_4 = 0.15,\ \sigma_5 = 0.43\}$. The initial conditions for the state variables are specified as $S_h(0) = 500,\ I_h(0) = 200,\ R_h(0) = 10,\ S_m(0) = 1000,\ I_m(0) = 100$.

It is worth noting that the selected noise intensity set Σ_1, together with the remaining model parameters, satisfies the conditions of Theorem (3). For this parameter regime, the basic reproduction number satisfies $R_0 > 1$ in the absence of control measures, that is, when $u_1 = 0,\ u_2 = 0$, indicating sustained dengue transmission.

The numerical results presented in Fig. 7(a) and dummyTXdummy- Fig. 7(e) demonstrate that the simultaneous implementation of both control strategies is highly effective in reducing the infected human population to a negligible level, while also substantially suppressing the mosquito population. The temporal profiles of the control variables are depicted in Fig. 7(c) and dummyTXdummy- Fig. 7(d), illustrating the optimal intensity and duration of intervention over the control horizon.

The associated cost functional incorporates the disease burden due to dengue infection, the costs of medical treatment, and the expenses related to awareness campaigns, environmental sanitation, and other preventive measures. As shown in Fig. 7(b), the total cost is significantly reduced when both control measures are applied, even after accounting for the implementation costs of the controls themselves.

The plots presented in Fig. 8 illustrate the effectiveness and relative importance of individual and combined control strategies in mitigating dengue transmission while minimizing the associated costs. In particular, Fig. 8(a) depicts the optimal profile of the awareness and prevention control u_1 under different scenarios, namely, in the absence and presence of the treatment control u_2. It is observed that, when u_2 is absent, the control u_1 must be applied over a longer duration to successfully suppress dengue transmission and restore the system toward a controlled state. A similar behavior is observed for the treatment control u_2 when applied individually in the absence of u_1, a longer or more intensive intervention is required compared to the case when both controls are implemented simultaneously as shown in Fig. 8(b). These results indicate that reliance on a single intervention places a greater burden on that control mechanism to compensate for the absence of the complementary strategy.

As shown in Fig. 8(d), the treatment control u_2 is more effective than the awareness-based control u_1 in reducing the infected human population when applied alone. However, the cost associated with the individual application of u_2 is slightly higher than that of u_1, reflecting the increased expenses related to medical treatment and case management. In contrast, the simultaneous implementation of both controls yields the lowest overall cost and requires a shorter duration of intervention, as illustrated in Fig. 8(a) to Fig. 8(c).

Consequently, the optimal outcome characterized by the minimum infected population size at the lowest total cos is achieved when the awareness and prevention control u_1 and the treatment control u_2 are applied concurrently, as demonstrated in Fig. 8.

8. Conclusion

In this work, we have developed a comprehensive stochastic framework to investigate dengue transmission dynamics under the combined influence of media modulated infection rates, nonlinear treatment responses, and environmental uncertainty. The study begins with the formulation of a stochastic dengue model that captures random perturbations arising from environmental and demographic variability. Rigorous mathematical analysis established the existence, uniqueness, and global positivity of solutions, ensuring the biological and analytical well posedness of the proposed system.

To ensure epidemiological relevance, the deterministic model is calibrated using reported data on dengue incidence from Rio de Janeiro, Brazil for the year 2024. The estimated parameters lie within biologically plausible ranges, and uncertainty is quantified through confidence and prediction intervals that account for data variability. These results support the model's consistency with observed trends and provide a reliable basis for the validity of the subsequent stochastic analysis, as well as for understanding disease dynamics and informing control strategies. The PRCC sensitivity analysis of R_0 reveals that transmission intensity is primarily driven by demographic and entomological factors that regulate host availability and vector-host contact. In particular, increased human recruitment (A_h), mosquito bite activity (α), transmission probabilities between humans and mosquitoes (β, β_m), mosquito maturation rate (δ), and environmental carrying capacity (K) improve viral circulation by increasing both the frequency of infectious contacts and vector abundance. In contrast, higher mosquito mortality (d_m), human mortality, and media driven awareness (η) suppress dengue transmission by reducing vector survival, infectious host availability, and effective human-mosquito interactions. Notably, media modulated awareness emerges as a critical intervention, as awareness induced behavioral changes such as personal protection and environmental management substantially reduce transmission potential and contribute to sustained outbreak prevention.

Stochastic perturbations play a significant role in shaping dengue transmission dynamics by influencing both disease persistence and extinction. Our analysis shows that, under certain conditions, stochastic trajectories fluctuate around their deterministic counterparts, indicating that the deterministic model can still approximate average system behavior in the presence of small environmental variability.

From a biological perspective, the results demonstrate that when the reproduction thresholds satisfy $R_0^h < 1$ or $R_0^m < 1$, the infection dies out in the human or mosquito population, respectively. These thresholds represent critical control targets, implying that reducing transmission in either population can be sufficient to interrupt disease spread. Importantly, the study reveals that increasing the intensity of environmental noise can drive both infected human and mosquito populations to extinction even when the deterministic basic reproduction number exceeds unity ($R_0 > 1$). This highlights a key biological insight: environmental variability such as fluctuations in temperature, rainfall, or vector habitats etc. can suppress transmission and potentially accelerate disease elimination beyond what is predicted by deterministic models. Although extinction thresholds indicate theoretical disease control, the presence of stochastic fluctuations in real transmission dynamics highlights the need for robust intervention strategies.

To address these challenges, a stochastic optimal control framework incorporates awareness based interventions (u_1) and treatment strategies (u_2). The results indicate that the combined implementation of both controls substantially reduces infected human and mosquito populations while achieving disease suppression at minimal overall cost. When applied jointly, both controls require shorter implementation periods and produce more effective results than when used individually. Although treatment alone achieves

a stronger immediate reduction in infections, it incurs higher costs, whereas awareness based interventions offer cost-efficient transmission reduction. The integrated strategy emerges as the most effective approach, minimizing infection burden and control costs simultaneously, and highlights the importance of coordinated public health responses under resource limitations.

In general, the results demonstrate that dengue transmission is governed by a complex interplay of nonlinear dynamics, stochastic effects, and behavioral responses. The proposed framework provides practical and quantitative insights for designing robust, cost effective, and adaptive dengue control strategies that integrate public awareness and medical interventions under uncertainty. By explicitly accounting for environmental variability and resource limitations, the findings support informed decision making for outbreak preparedness and efficient resource allocation. This work lays a foundation for future extensions incorporating spatial heterogeneity, intermediate hosts, time delays, age structured populations, or data driven stochastic parameter estimation to further enhance real-world applicability.

CRediT authorship contribution statement

Anita Mandal: Conceptualization, Visualization, Funding acquisition, Methodology, Formal analysis, Software, Writing – original draft; **Moumita Ghosh:** Conceptualization, Methodology, Formal analysis, Investigation, Software, Visualization, Writing – review & editing; **Subhash C. Bagui:** Validation, Writing – review & editing; **Pritha Das:** Methodology, Writing – review & editing; **Dibakar Ghosh:** Conceptualization, Visualization, Supervision, Writing – review & editing; **Matjaž Perc:** Conceptualization, Visualization, Supervision, Writing – review & editing.

Data availability

The weekly dengue incidence data for Rio de Janeiro, Brazil, used in this study are obtained from Brazil's Notifiable Diseases Information System (SINAN) for the year 2024. These data are publicly available and can be accessed through the SINAN database at http://tabnet.datasus.gov.br/.

Declaration of competing interest

With reference to the study, the authors claim that they have no conflicts of interest.

Acknowledgements

A. M. is thankful to the University Grants Commission (UGC), Government of India, for providing fellowship, with NTA Ref. No.: 221610033737. M.P. is supported by the Slovenian Research and Innovation Agency (Grant No. P1-0403).

Appendix A.

This appendix presents the derivation of the disease-free equilibrium and R_0 for the deterministic counterpart of the model, establishing the threshold condition for disease invasion or extinction.

Disease free equilibrium: The disease-free equilibrium represents the state in which the infection is absent from both the human and mosquito populations. To determine the disease-free equilibrium of the deterministic counterpart of system (1), we set the infected compartments to zero, i.e., $I_h = I_m = 0$, and solve the remaining system of equations. Substituting these conditions into the model yields the disease-free equilibrium, denoted by $E_0 = \left(S_h^0,\ I_h^0,\ R_h^0,\ S_m^0,\ I_m^0\right) = \left(\frac{A_h}{d_h},\ 0,\ 0,\ K\left(1 - \frac{d_m}{\delta}\right),\ 0\right)$ which exists in the biologically feasible region, provided that $\delta > d_m$.

- **Basic reproduction number(R_0):** The basic reproduction number, R_0, represents the expected number of secondary infections generated by a single infectious individual in a fully susceptible population. It indicates that if $R_0 > 1$, the disease can spread; if $R_0 < 1$, it will eventually die out. For vector-borne diseases such as dengue, which is transmitted between humans and mosquitoes, calculating R_0 helps us to understand the potential for outbreaks, identify the most influential transmission parameters, which guide public health interventions.

  The basic reproduction number (R_0) is derived by spectral analysis of the next generation matrix, obtained by decomposing the system into a subsystem as $\frac{dX}{dt} = (\mathcal{F} - \mathcal{V})$, where $\mathbf{X} = \left[I_h, I_m\right]^{\mathrm{T}}$. Here,

  $\mathcal{F} = \begin{bmatrix} \alpha\left(\beta - \frac{\beta_1\eta}{\beta_2+\eta}\right) S_h I_m \\ \alpha\beta_m S_m I_h \end{bmatrix}$, $\mathcal{V} = \begin{bmatrix} (r_h + d + d_h) I_h + \frac{aI_h^2}{(bI_h^2 + cI_h + 1)} \\ d_m I_m \end{bmatrix}$ represent the rate of new infections and the rate of transfer between compartments, respectively. For the infected subsystem, we construct the Jacobian matrices $F = \left[\frac{\partial \mathcal{F}_i}{\partial X_j}\right]$ and $V = \left[\frac{\partial \mathcal{V}_i}{\partial X_j}\right]$, evaluated at E_0 given by

  $F = \begin{bmatrix} 0 & \alpha\left(\beta - \frac{\beta_1\eta}{\beta_2+\eta}\right) S_h^0 \\ \alpha\beta_m S_m^0 & 0 \end{bmatrix}$, $V = \begin{bmatrix} (r_h + d + d_h) & 0 \\ 0 & d_m \end{bmatrix}$.

So, the spectral radius of the matrix FV^{-1} yields

$$R_0 = \sqrt{\frac{\alpha^2 A_h \beta_m K(\delta - d_m)\left(\beta - \frac{\beta_1 \eta}{\beta_2 + \eta}\right)}{d_m d_h \delta (r_h + d + d_h)}}. \tag{A.1}$$

This derived expression for R_0 characterizes the transmission potential of the disease and forms the basis for subsequent sensitivity and control analysis.

Appendix B.

Existence of endemic equilibrium: To establish the existence of the endemic equilibrium, denoted by $E_1 = \left(S_h^*,\ I_h^*,\ R_h^*,\ S_m^*,\ I_m^*\right)$, we analyze the deterministic counterpart of system (1) by setting the time derivatives equal to zero. The endemic equilibrium is characterized by persistent infection in both host and vector populations, requiring $I_h^* > 0$ and $I_m^* > 0$. Through algebraic manipulation of the equilibrium equations, we derive the following

$$S_h^* = \frac{\delta\left(r_h + d + d_h + \frac{aI_h^*}{bI_h^{*2} + cI_h^* + 1}\right)(\alpha\beta_m I_h^* + d_m)}{\alpha^2\ K\beta_m\left(\beta - \frac{\beta_1\eta}{\beta_2+\eta}\right)(\delta - d_m)},\ R_h^* = \frac{1}{d_h}\left(r_h I_h^* + \frac{aI_h^{*2}}{bI_h^{*2} + cI_h^* + 1}\right)$$

$$S_m^* = \frac{Kd_m}{\delta}\left(\frac{\delta - d_m}{\alpha\beta_m I_h^* + d_m}\right),\ I_m^* = \frac{K\alpha\beta_m I_h^*}{\delta}\left(\frac{\delta - d_m}{\alpha\beta_m I_h^* + d_m}\right).$$

Replacing the above values in the equation for $\dot{S_h}$, we obtain an equation in terms of I_h^* as

$$A_h - \left(r_h + d + d_h + \frac{aI_h^*}{bI_h^{*2} + cI_h^* + 1}\right)\left(I_h^* + \frac{\delta d_h \alpha\beta_m I_h^* + \delta d_h d_m}{K\alpha^2\beta_e\beta_m(\delta - d_m)}\right) = 0 \tag{B.1}$$

Let us now define a continuous function $f : [0, \infty) \to \mathbb{R}$ as follows

$$f(I_h) = A_h - \left(r_h + d + d_h + \frac{aI_h}{bI_h{}^2 + cI_h + 1}\right)\left(I_h + \frac{\delta d_h \alpha\beta_m I_h + \delta d_h d_m}{K\alpha^2\beta_e\beta_m(\delta - d_m)}\right) \tag{B.2}$$

Now,

$$\lim_{I_h \to 0} f(I_h) = A_h - \frac{\delta d_h d_m (r_h + d + d_h)}{K\alpha^2\beta_e\beta_m(\delta - d_m)} = A_h\left(1 - \frac{1}{R_0^2}\right) > 0, \qquad \text{for} \quad R_0 > 1.$$

$$\lim_{I_h \to \infty} f(I_h) = -\infty.$$

By the intermediate value theorem, since $f(I_h)$ is continuous, there exists at least one positive root I_h^* such that $f(I_h^*) = 0$. Consequently, the existence of this positive solution $I_h^* > 0$ ensures that S_h^*, R_h^*, S_m^* and I_m^* also attain positive values, as expressed in their respective formulations. Therefore, for $R_0 > 1$, the deterministic system admits an endemic equilibrium characterized by the persistence of infection ($I_h^* > 0$) as described in Eq. (B.1).

Appendix C.

This appendix provides the proof of Theorem (2). The approach is based on constructing a suitable Lyapunov function and applying Itô's formula to analyze the stochastic stability of the system around the disease-free equilibrium. To establish the result, we introduce the following Lyapunov function, which measures the deviation of the system from the disease-free equilibrium. Accordingly, define $V_1 : \mathbb{R}_+^5 \to \mathbb{R}_+$ as follows:

$$V_1\left(S_h, I_h, R_h, S_m, I_m\right) = \frac{1}{2}\left(S_h - S_h^0\right)^2 + I_h + R_h + \frac{1}{2}\left(S_m - S_m^0\right)^2 + I_m \tag{C.1}$$

Using Itô's formula on V_1 we get,

$$\begin{aligned} dV_1\left(S_h, I_h, R_h, S_m, I_m\right) = LV_1\left(S_h, I_h, R_h, S_m, I_m\right)dt + \sigma_1 S_h\left(S_h - S_h^0\right)dW_1 + \sigma_2 I_h dW_2 + \sigma_3 R_h dW_3 \\ + \sigma_4 S_m\left(S_m - S_m^0\right)dW_4 + \sigma_5 I_m dW_5 \end{aligned} \tag{C.2}$$

where,

$$\begin{aligned} LV_1 &= \left[\left(S_h - S_h^0\right)\left(A_h - \alpha\beta_e S_h I_m - d_h S_h\right) + \left(\alpha\beta_e S_h I_m - r_h I_h - \frac{aI_h^2}{bI_h^2 + cI_h + 1} - dI_h - d_h I_h\right)\right. \\ &\quad + \left(r_h I_h + \frac{aI_h^2}{bI_h^2 + cI_h + 1} - d_h R_h\right) + \left(\alpha\beta_m S_m I_h - d_m I_m\right) \\ &\quad \left. + \left(S_m - S_m^0\right)\left(\delta\left(1 - \frac{S_m + I_m}{K}\right)(S_m + I_m) - \alpha\beta_m S_m I_h - d_m S_m\right)\right] + \frac{1}{2}\left(\sigma_1^2 S_h^2 + \sigma_4^2 S_m^2\right) \\ &\le -\left(d_h\left(S_h - S_h^0\right)^2 + d_m\left(d + d_h + r_h\right)\left(1 - R_0^2\right)I_h + d_h R_h + d_m\left(S_m - S_m^0\right)^2 + d_m I_m\right) \\ &\quad + A_h S_h + \alpha\beta_e S_h I_m(S_h^0 + 1) + \delta S_m^2 + \alpha\beta_m S_m I_h(S_m^0 + 1) + \frac{1}{2}\left(\sigma_1^2 S_h^2 + \sigma_4^2 S_m^2\right) \\ &\le -\left(d_h\left(S_h - S_h^0\right)^2 + d_m\left(d + d_h + r_h\right)\left(1 - R_0^2\right)I_h + d_h R_h + d_m\left(S_m - S_m^0\right)^2 + d_m I_m\right) \\ &\quad + \frac{A_h}{d_h}\left(A_h + \alpha\beta_e K(S_h^0 + 1) + \alpha\beta_m K(S_m^0 + 1)\right) + \frac{1}{2}\left(\sigma_1^2 S_h^2 + \sigma_4^2 S_m^2 + 2\delta K^2\right) \end{aligned} \tag{C.3}$$

Integrating both sides of (C.2) from 0 to t and using (C.3), then taking the expectation we get,

$$\begin{aligned} 0 \le \mathbb{E}V_1(t) - V_1(0) &= \mathbb{E}\int_0^t LV_1(s)ds \\ &\le -\mathbb{E}\int_0^t \left[d_h\left(S_h(s) - S_h^0\right)^2 + d_m(d + d_h + r_h)(1 - R_0^2)I_h(s) + d_h R_h(s)\right. \\ &\quad \left. + d_m\left(S_m(s) - S_m^0\right)^2 + d_m I_m(s)\right]ds + \frac{1}{2}\left(\frac{A_h^2\sigma_1^2}{d_h^2} + \sigma_4^2 K^2 + 2\delta K^2\right)t \\ &\quad + \left[\frac{A_h}{d_h}\left(A_h + pK(S_h^0 + 1) + r_h + \alpha\beta_m K(S_m^0 + 1)\right)\right]t \end{aligned}$$

Therefore,

$$\begin{aligned} &\lim_{t\to\infty} \mathbf{Sup}\frac{1}{t}\mathbb{E}\int_0^t \left[d_h\left(S_h - S_h^0\right)^2 + d_m(d + d_h + r_h)(1 - R_0^2)I_h + d_h R_h + d_m\left(S_m - S_m^0\right)^2 + d_m I_m\right] \\ &\qquad \le \frac{A_h}{d_h}\left(A_h + \alpha\beta_e K(S_h^0 + 1) + r_h + \alpha\beta_m K(S_m^0 + 1)\right) + \frac{1}{2}\left(\frac{A_h^2\sigma_1^2}{d_h^2} + \sigma_4^2 K^2 + 2\delta K^2\right) \end{aligned}$$

This completes the proof. The result shows that stochastic perturbations do not destabilize the disease-free equilibrium when $R_0 < 1$, and system trajectories fluctuating around it in the long run.

Appendix D.

This appendix establishes the proof of Theorem (3), focusing on the stochastic behavior of the system around the endemic equilibrium under the given conditions. The analysis accounts for the combined effect of persistence ($R_0 > 1$) and bounded stochastic fluctuations. To proceed, we introduce a Lyapunov function that quantifies deviations from the endemic equilibrium. Accordingly, define a function $V : \mathbb{R}_+^5 \to \mathbb{R}_+$ as follows:

$$V(S_h, I_h, R_h, S_m, I_m) = V_1 + V_2 \tag{D.1}$$

$$\text{where,} \quad V_1 = \frac{1}{2}\left(S_h - S_h^* + I_h - I_h^* + R_h - R_h^*\right)^2 \quad \text{and} \quad V_2 = \frac{1}{2}\left(S_m - S_m^* + I_m - I_m^*\right)^2$$

Using Itô's formula on V_1 we get,

$$\begin{aligned} dV\left(S_h, I_h, R_h, S_m, I_m\right) &= \left(LV_1 + LV_2\right)\left(S_h, I_h, R_h, S_m, I_m\right)dt + \left(S_h - S_h^* + I_h - I_h^* + R_h - R_h^*\right) \\ &\quad \left(\sigma_1 S_h dW_1 + \sigma_2 I_h dW_2 + \sigma_3 R_h dW_3\right) + \left(S_m - S_m^* + I_m - I_m^*\right)\left(\sigma_4 S_m dW_4 + \sigma_5 I_5 dW_5\right) \end{aligned} \tag{D.2}$$

where,

$$\begin{aligned}
LV_1 &= \Big(S_h - S_h^* + I_h - I_h^* + R_h - R_h^*\Big)\Big(A_h - d_h(S_h + I_h + R_h) - dI_h\Big) + \frac{1}{2}\Big(\sigma_1^2 S_h^2 + \sigma_2^2 I_h^2 + \sigma_3^2 R_h^2\Big)\\
&= \Big(S_h - S_h^* + I_h - I_h^* + R_h - R_h^*\Big)\Big[-d_h(S_h - S_h^*) - (d_h + d)(I_h - I_h^*) - d_h(R_h - R_h^*)\Big] + \frac{1}{2}\Big(\sigma_1^2 S_h^2 + \sigma_2^2 I_h^2 + \sigma_3^2 R_h^2\Big)\\
&\le \Big[-d_h\big(S_h - S_h^*\big)^2 - (d_h + d)\big(I_h - I_h^*\big)^2 - d_h\big(R_h - R_h^*\big)^2\Big] + (2d_h + d)(S_h I_h^* + I_h S_h^*)\\
&\quad + 2d_h(S_h R_h^* + R_h S_h^*) + (2d_h + d)(I_h R_h^* + R_h I_h^*) + \frac{1}{2}\Big(\sigma_1^2 S_h^2 + \sigma_2^2 I_h^2 + \sigma_3^2 R_h^2\Big)\\
&\le \Big[-d_h\big(S_h - S_h^*\big)^2 - (d_h + d)\big(I_h - I_h^*\big)^2 - d_h\big(R_h - R_h^*\big)^2\Big] + \frac{A_h}{d_h}(2d_h + d)(S_h^* + 2I_h^* + R_h^*)\\
&\quad + 2A_h(R_h^* + S_h^*) + \frac{A_h^2}{2d_h^2}(\sigma_1^2 + \sigma_2^2 + \sigma_3^2)
\end{aligned} \tag{D.3}$$

and

$$\begin{aligned}
LV_2 &= \Big(S_m - S_m^* + I_m - I_m^*\Big)\left(\delta\Big(1 - \frac{S_m + I_m}{K}\Big)(S_m + I_m) - d_m(S_m + I_m)\right) + \frac{1}{2}\Big(\sigma_4^2 S_m^2 + \sigma_5^2 I_m^2\Big)\\
&= \Big(S_m - S_m^* + I_m - I_m^*\Big)\left(\delta\Big(1 - \frac{S_m + I_m}{K}\Big)(S_m + I_m) - \frac{\delta S_m^*\Big(1 - \frac{S_m^* + I_m^*}{K}\Big)(S_m + I_m)\Big)}{S_m^* + I_m^*}\right) + \frac{1}{2}\Big(\sigma_4^2 S_m^2 + \sigma_5^2 I_m^2\Big)\\
&= \frac{\delta}{S_m^* + I_m^*}\left(I_m^* - \frac{(S_m^* + I_m^*)(S_m + I_m)}{K}\right)(S_m - S_m^*)^2 - \frac{\delta S_m^*}{S_m^* + I_m^*}(I_m - I_m^*)^2\\
&\quad + \frac{\delta}{S_m^* + I_m^*}\Big[-S_m^* + I_m^* - \frac{(S_m^* + I_m^*)(S_m + I_m)}{K}\Big]\Big(S_m - S_m^*\Big)(I_m - I_m^*\Big) + \frac{1}{2}\Big(\sigma_4^2 S_m^2 + \sigma_5^2 I_m^2\Big)\\
&\le -\frac{\delta S_m^*}{S_m^* + I_m^*}(S_m - S_m^*)^2 - \frac{\delta S_m^*}{S_m^* + I_m^*}(I_m - I_m^*)^2 + \frac{2\delta S_m^*}{S_m^* + I_m^*}\Big(S_m^* I_m + S_m I_m^*\Big) + \frac{1}{2}\Big(\sigma_4^2 S_m^2 + \sigma_5^2 I_m^2\Big)\\
&\le -\frac{\delta S_m^*}{S_m^* + I_m^*}(S_m - S_m^*)^2 - \frac{\delta S_m^*}{S_m^* + I_m^*}(I_m - I_m^*)^2 + \frac{1}{2d_m}S_m^* K\delta^2 + \frac{K^2}{2}\Big(\sigma_4^2 + \sigma_5^2\Big)
\end{aligned} \tag{D.4}$$

Using (D.3) and (D.4) and then integrating both sides of (D.2) from 0 to t, followed by taking expectations, we obtain,

$$\begin{aligned}
0 \le \mathbb{E}V(t) - V(0) &= \mathbb{E}\int_0^t \Big(LV_1(s) + LV_2(s)\Big)ds\\
&\le -\mathbb{E}\int_0^t \left[d_h\big(S_h - S_h^*\big)^2 + (d + d_h)\big(I_h - I_h^*\big)^2 + d_h\big(R_h - R_h^*\big)^2\right.\\
&\quad \left. + \frac{\delta S_m^*}{(S_m^* + I_m^*)}\Big(\big(S_m - S_m^*\big)^2 + \big(I_m - I_m^*\big)^2\Big)\right] + \left[\frac{A_h}{d_h}(2d_h + d)(S_h^* + 2I_h^* + R_h^*)\right.\\
&\quad \left. + 2A_h(R_h^* + S_h^*) + \frac{1}{2d_m}S_m^* K\delta^2 + \frac{A_h^2}{2d_h^2}(\sigma_1^2 + \sigma_2^2 + \sigma_3^2) + \frac{K^2}{2}(\sigma_4^2 + \sigma_5^2)\right]t
\end{aligned}$$

Therefore,

$$\begin{aligned}
&\lim_{t\to\infty} \mathbf{Sup}\frac{1}{t}\mathbb{E}\int_0^t \left[d_h\big(S_h - S_h^*\big)^2 + (d + d_h)\big(I_h - I_h^*\big)^2 + d_h\big(R_h - R_h^*\big)^2 + \frac{\delta S_m^*}{(S_m^* + I_m^*)}\Big(\big(S_m - S_m^*\big)^2 + \big(I_m - I_m^*\big)^2\Big)\right]\\
&\qquad \le \frac{A_h}{d_h}(2d_h + d)(S_h^* + 2I_h^* + R_h^*) + 2A_h(R_h^* + S_h^*) + \frac{1}{2d_m}S_m^* K\delta^2 + \frac{A_h^2}{2d_h^2}(\sigma_1^2 + \sigma_2^2 + \sigma_3^2) + \frac{K^2}{2}(\sigma_4^2 + \sigma_5^2)
\end{aligned}$$

This completes the proof. The result indicates that for $R_0 > 1$ and sufficiently small noise intensity relative to the natural death rate, the system remains close to the endemic equilibrium, ensuring stochastic persistence of the disease.

Appendix E.

To prove the extinction result stated in Theorem (4), we analyze the stochastic dynamics of the infected compartments in both the host and vector populations. In particular, we derive sufficient conditions under which the infected populations decay exponentially to zero almost surely. By applying Itô's formula to the last equation of system (1), we obtain

$$d\big(\log I_m(t)\big) = \left[\frac{\alpha\beta_m S_m I_h}{I_m} - d_m\right]dt - \frac{\sigma_5^2}{2}dt + \sigma_5 dW_5 \ \le \left[\alpha\beta_m S_m I_h - d_m\right]dt - \frac{\sigma_5^2}{2}dt + \sigma_5 dW_5$$

$$\leq \left[\frac{A_h\alpha\beta_m K}{d_h} - d_m - \frac{\sigma_5^2}{2}\right]dt + \sigma_5 dW_5$$

Integrating the expression from 0 to t, and subsequently dividing by t yields:

$$\begin{aligned}\frac{\log I_m(t)}{t} &\leq \left[\frac{A_h\alpha\beta_m K}{d_h} - d_m - \frac{\sigma_5^2}{2}\right] + \frac{1}{t}\int_0^t \sigma_5 dW_5(\tau)d\tau + \frac{\log I_m(0)}{t} \\ &\leq d_m(R_0^m - 1) + \frac{1}{t}\sigma_5 W_5(t) + \frac{\log I_m(0)}{t}\end{aligned} \tag{E.1}$$

Using strong law of large numbers for Martingale, we have

$$\lim_{t\to\infty}\frac{1}{t}\sigma_5 W_5(t) = 0, \qquad \textbf{a.s.}$$

Now, taking limit superior as $t \to \infty$ in both sides of (E.1), we get

$$\lim_{t\to\infty}\textbf{Sup}\frac{\log I_m(t)}{t} \leq d_m(R_0^m - 1) \qquad \textbf{a.s.}$$

which implies that if $R_0^m < 1$, then

$$\lim_{t\to\infty}\textbf{Sup}\frac{\log I_m(t)}{t} < 0 \qquad \textbf{a.s.} \implies \lim_{t\to\infty} I_m(t) = 0 \qquad \textbf{a.s.}$$

meaning that the infected mosquito population will die out almost surely (a.s.) if $R_0^m < 1$.

Similarly, by applying Itô's formula to the second equation of model (1), we have

$$\begin{aligned}d\log I_h(t) &= \left[\frac{\alpha\left(\beta - \frac{\beta_1\eta}{\beta_2+\eta}\right)S_h I_m}{I_h} - (d + d_h + r_h) - \frac{aI_h}{bI_h^2 + cI_h + 1}\right]dt - \frac{\sigma_2^2}{2}dt + \sigma_2 dW_2 \\ &\leq \left[\frac{A_h K\alpha\left(\beta - \frac{\beta_1\eta}{\beta_2+\eta}\right)}{d_h} - (d + d_h + r_h) - \frac{a}{(2\sqrt{b} + c)} - \frac{\sigma_2^2}{2}\right]dt + \sigma_2 dW_2\end{aligned} \tag{E.2}$$

Integrating the Eq. (E.2) from 0 to t and then dividing it by t yields

$$\begin{aligned}\frac{\log I_h(t)}{t} &\leq \left[\frac{A_h K\alpha\left(\beta - \frac{\beta_1\eta}{\beta_2+\eta}\right)}{d_h} - (d + d_h + r_h) - \frac{a}{(2\sqrt{b} + c)} - \frac{\sigma_2^2}{2}\right] + \frac{1}{t}\int_0^t \sigma_2 dW_2(\tau)d\tau + \frac{\log I_h(0)}{t} \\ &\leq (d + d_h + r_h)(R_0^h - 1) + \frac{1}{t}\sigma_2 W_2(t) + \frac{\log I_h(0)}{t}\end{aligned} \tag{E.3}$$

According to the well-known law of large numbers for local martingales, we derive the following equation as

$$\lim_{t\to\infty}\frac{1}{t}\sigma_2 W_2(t) = 0, \qquad \textbf{a.s.}$$

Now taking limit superior as $t \to \infty$ in both sides of (E.3), we get

$$\lim_{t\to\infty}\textbf{Sup}\frac{\log I_h(t)}{t} \leq d_m(R_0^h - 1) < 0 \qquad \textbf{a.s.} \qquad \textbf{if } R_0^h < 1$$

This implies the extinction of $I_h(t)$, i.e., $\lim_{t\to\infty} I_h(t) = 0$ with probability 1 for $R_0^h < 1$.

This establishes that the infected populations $I_h(t)$, and $I_m(t)$, converge to zero exponentially as $t \to \infty$ with probability one under either of the stated conditions. Hence, the disease becomes extinct in both the host and vector populations whenever $R_0^h < 1$ or $R_0^m < 1$. This completes the proof.

References

[1] W.H. Organization, Dengue and severe dengue, 2024. https://www.who.int/emergencies/disease-outbreak-news/item/2024-DON518.

[2] S.B. Halstead, Dengue, The Lancet 370 (9599) (2007) 1644–1652. https://doi.org/10.1016/s0140-6736(07)61687-0

[3] L.C. Katzelnick, L. Gresh, M.E. Halloran, J.C. Mercado, G. Kuan, A. Gordon, Antibody-dependent enhancement of severe dengue disease in humans, Science 358 (6365) (2017) 929–932. https://doi.org/10.1126/science.aan6836

[4] L. Esteva, C. Vargas, Analysis of a dengue disease transmission model, Math. Biosci. 150 (2) (1998) 131–151. https://doi.org/10.1016/S0025-5564(98)10003-2

[5] M. Derouich, A. Boutayeb, E. Twizell, A Model Dengue Fever 2 (2003) 4. https://doi.org/10.1186/1475-925x-2-4

[6] D. Murillo, A. Murillo, S. Lee, The role of vertical transmission in the control of dengue fever, Int. J. Environ. Res. Public Health 16 (2019) 803. https://doi.org/10.3390/ijerph16050803

[7] Y. Wang, S. Zhao, Y. Wei, K. Li, X. Jiang, C. Li, C. Ren, S. Yin, J. Ho, J. Ran, Impact of climate change on dengue fever epidemics in south and southeast asian settings: A modelling study, Infectious Disease Modell. 8 (3) (2023) 645–655. https://doi.org/10.1016/j.idm.2023.05.008

[8] Y. Wang, Y. Wei, K. Li, X. Jiang, C. Li, Q. Yue, B.C.Y. Zee, K.C. Chong, Impact of extreme weather on dengue fever infection in four asian countries: A modelling analysis, Environ. Int. 169 (2022) 107518. https://doi.org/10.1016/j.envint.2022.107518

[9] J. Xiang, A. Hansen, Q. Liu, X. Liu, M.X. Tong, Y. Sun, S. Cameron, S. Hanson-Easey, G.-S. Han, C. Williams, P. Weinstein, P. Bi, Association between dengue fever incidence and meteorological factors in guangzhou, china, Environm. Res. 153 (2005) 17–26. https://doi.org/10.1016/j.envres.2016.11.009

[10] A.R. Kaye, W.S. Hart, J. Bromiley, S. Iwami, R.N. Thompson, A direct comparison of methods for assessing the threat from emerging infectious diseases in seasonally varying environments, J. Theoretical Biol. 548 (2022) 111195. https://doi.org/10.1016/j.jtbi.2022.111195
[11] S. Ghosh, M. Banerjee, A.K. Chattopadhyay, Effect of vaccine dose intervals: Considering immunity levels, vaccine efficacy, and strain variants for disease control strategy, PLoS One 19 (9) (2024) 310152. https://doi.org/10.1371/journal.pone.0310152
[12] L. Liu, X. Chen, A. Szolnoki, Coevolutionary dynamics via adaptive feedback in collective-risk social dilemma game, Elife 12 (2023) 82954. https://doi.org/10.7554/eLife.82954
[13] A. Szolnoki, Z. Wang, M. Perc, Wisdom of Groups Promotes Cooperation In Evolutionary Social Dilemmas 2 (2012) 576. https://doi.org/10.1038/srep00576
[14] B. Mintz, F. Fu, Evolutionary multi-agent reinforcement learning in group social dilemmas, Chaos An Interdiscip. J. Nonlinear Sci. 35 (2) (2025). https://doi.org/10.1063/5.0246332
[15] K. Royce, F. Fu, Mathematically modeling spillovers of an emerging infectious zoonosis with an intermediate host, PloS one 15 (8) (2020) 237780. https://doi.org/10.1371/journal.pone.0237780
[16] C. Favier, D. Schmit, C. Müller-Graf, B. Cazelles, N. Degallier, B. Mondet, M.-A. Dubois, Influence of spatial heterogeneity on an emerging infectious disease: The case of dengue epidemics, Proc. Biol. Sci. The Royal Soc. 272 (2005) 1171–1177. https://doi.org/10.1098/rspb.2004.3020
[17] S. Dey, D.K. Das, S. Ghorai, M. Banerjee, Spatially heterogeneous eco-epidemic model: Stabilizing role of non-local disease transmission, Commun. Nonlinear Sci. Numerical Simul. 138 (2024) 108238. https://doi.org/10.1016/j.cnsns.2024.108238
[18] D.K. Das, S. Ghorai, M. Banerjee, Spatio-temporal dynamics of an sis model with nonlinear incidence and nonlocal disease transmission, Nonlinear Dynam. 111 (16) (2023) 15591–15612. https://doi.org/10.1007/s11071-023-08633-1
[19] A. Mandal, P. Debnath, P. Das, D. Ghosh, A climate-driven mechanistic model of dengue transmission: Linking entomological processes to epidemiological dynamics, Chaos Solit. Fract. 204 (2026) 117818. https://doi.org/10.1016/j.chaos.2025.117818
[20] Y.L. Hii, H. Zhu, N. Ng, L.C. Ng, J. Rocklöv, Forecast of dengue incidence using temperature and rainfall, PLoS Neglected Trop. Diseases 6 (2012) 1908. https://doi.org/10.1371/journal.pntd.0001908
[21] O. Mahmod, R. Indawati, A.A. Suleiman, M. Qomaruddin, R. Sokkalingam, Model forecasting development for dengue fever incidence in surabaya city using time series analysis, Processes 10 (2022) 2454. https://doi.org/10.3390/pr10112454
[22] Y.S. Kusuma, D. Burman, R. Kumari, A.S. Lamkang, B.V. Babu, Impact of health education based intervention on community's awareness of dengue and its prevention in delhi, india, Global Health Promot. 26 (1) (2019) 50–59. https://doi.org/10.1177/1757975916686912
[23] A. Misra, A. Sharma, J. Shukla, Modeling and analysis of effects of awareness programs by media on the spread of infectious diseases, Mathem. Computer Modell. 53 (5) (2011) 1221–1228. https://doi.org/10.1016/j.mcm.2010.12.005
[24] S.S. Musa, S. Qureshi, S. Zhao, A. Yusuf, U.T. Mustapha, D. He, Mathematical modeling of covid-19 epidemic with effect of awareness programs, Infectious Disease Modell. 6 (2021) 448–460. https://doi.org/10.1016/j.idm.2021.01.012
[25] M. Ghosh, A.K. Misra, P. Das, Analysis of a delayed miscr rumor spread model with refutation mechanism, The Europ. Phys. J. Plus 139 (6) (2024) 562. https://doi.org/10.1140/epjp/s13360-024-05339-0
[26] T. Li, Y. Xiao, Complex dynamics of an epidemic model with saturated media coverage and recovery, Nonlinear Dynam. 107 (2022) 2995–3023. https://doi.org/10.1007/s11071-021-07096-6
[27] Q. Pan, J. Huang, H. Wang, An sirs model with nonmonotone incidence and saturated treatment in a changing environment, J. Math. Biol. 85 (3) (2022) 23. https://doi.org/10.1007/s00285-022-01787-3
[28] L.J.S. Allen, An introduction to stochastic epidemic models, 1945, Springer, 2008. https://doi.org/10.1007/978-3-540-78911-6_3
[29] A. Din, Y. Li, Lévy noise impact on a stochastic hepatitis b epidemic model under real statistical data and its fractal-fractional atangana-baleanu order model, Phys. Scrip. 96 (12) (2021) 124008. https://doi.org/10.1088/1402-4896
[30] N. Mondal, S. Karmakar, G. Samanta, Predator prey dynamics with nonlinear prey refuge, additional food and specific predator mortality in deterministic and stochastic environments, Stochastic Environm. Res. Risk Assessment 39 (2025) 6435–6462. https://doi.org/10.1007/s00477-025-03106-w
[31] A. Din, T. Khan, Y. Li, H. Tahir, A. Khan, W.A. Khan, Mathematical analysis of dengue stochastic epidemic model, Results Phys. 20 (2021) 103719. https://doi.org/10.1016/j.rinp.2020.103719
[32] N. Dalal, D. Greenhalgh, X. Mao, A stochastic model of aids and condom use, J. Math. Anal. Appl. 325 (2007) 36–53. https://doi.org/10.1016/j.jmaa.2006.01.055
[33] X. Mao, G. Marion, E. Renshaw, Environmental brownian noise suppresses explosions in population dynamics, in: Stochastic Processes and their Applications, 2002, pp. 95–110. https://doi.org/10.1016/S0304-4149(01)00126-0
[34] M.S. Khatun, K.B. Mahato, P. Das, Dynamics of an susav ir epidemic model with stochastic optimal control and awareness programs, Chaos Solit. Fract. 183 (2024) 114898. https://doi.org/10.1016/j.chaos.2024.114898
[35] R.P. Agarwal, Q. Badshah, G. Rahman, S. Islam, Optimal control & dynamical aspects of a stochastic pine wilt disease model, J. Franklin Inst. 356 (7) (2019) 3991–4025. https://doi.org/10.1016/j.jfranklin.2019.03.007
[36] X. Zhou, X. Shi, M. Wei, Dynamical behavior and optimal control of a stochastic mathematical model for cholera, Chaos, Solitons & Fractals 156 (2022) 111854. https://doi.org/10.1016/j.chaos.2022.111854
[37] M. Ishikawa, Stochastic optimal control of an sir epidemic model with vaccination, in: Proceedings of the ISCIE International Symposium on Stochastic Systems Theory and its Applications, the ISCIE International Symposium on Stochastic Systems Theory and its Applications, 2012, pp. 57–62. https://doi.org/10.5687/sss.2012.57
[38] X. Mao, Stochastic Differential Equations and Applications, 2nd Edition, Woodhead Publishing, 2007. https://doi.org/10.1533/9780857099402
[39] M. Ghosh, S. Das, P. Das, Dynamics and control of delayed rumor propagation through social networks, J. Appl. Math. Comput. 68 (5) (2022) 3011–3040. https://doi.org/10.1007/s12190-021-01643-5
[40] M. Ghosh, P. Das, Analysis of online misinformation spread model incorporating external noise and time delay and control of media effort, Diff. Eq. Dynam. Syst. 33 (1) (2025) 261–301. https://doi.org/10.1007/s12591-023-00657-8